MAY- AUG. 2005
Volume XI Number II
ISSN 0859 144X

THE ASEAN JOURNAL OF RADIOLOGY

Published by The Radiological Society and
The Royal College of Radiologists of Thailand,
Bangkok, Thailand

Started through an educational grant from Bracco since 1995

THE IMAGE OF INNOVATION

MAY - AUG. 2005
Volume XI Number II
ISSN 0859 144X

THE ASEAN JOURNAL OF RADIOLOGY

Published by The Radiological Society and
The Royal College of Radiologists of Thailand,
Bangkok, Thailand

Started through an educational grant from Bracco since 1995

Chief Editor

Professor Kawee Tungsubutra
Kaweevej Hospital, 318 Taksin Road, Dhonburi, Bangkok 10600, Thailand.

Asean Journal of Radiology.
Instructions for Authors.

1. The Asean Journal of Radiology publishes the papers on Radiological Sciences, such as research work, review articles, case reports, innovations in Medical Sciences related to all branches of Radiology, and letters to the editor. The aforementioned materials can be written in English only.

2. The authors have to submit 2 copies of the manuscript and a diskette: **to Prof. Dr. Kawee Tungsubutra.** 318 Kaweevej Hospital, Tarksin Road, Dhonburi, Bangkok 10600, Thailand.

3. The original copy to be submitted must be typed in a double space on one side of the page of 8.1/2" x 11.1/2" paper.

4. The format of the article must include :
   a. Title page and address of the author (s)
   b. Abstract
   c. Introduction (Background)
   d. Material and Method
   e. Results and discussion (Tables and Illustrations)
   f. Acknowledgement (if any)
   g. References (Follow the Vancouver style developed by ICMJE)

5. We will provide 5 copies of reprints for the author (s) who submit (s) an article for publication in the Asean Journal.

6. The illustrations and tables must be clearly prepared with legends in English as they are the art works to be reproduced.

7. The authors are reponsible for the contents of the article as to its facts and findings.

8. Ethics.

Paper reporting studies which might be interpreted as human experimentation (e.g. controlled trials) should conform to the standards of the Declaration of Helsinki (see British Medical Journal 1964: 2: 177) and should indicate that, approval that such studies may proceed, has been granted by the local or hospital Ethics Committee.

When reporting experiments on animals indicate whether the institution's or the National Research Council's guide for, or any national law on, the care and use of laboratory animals was followed.

THE ASEAN JOURNAL OF RADIOLOGY

Volume XI Number II MAY-AUG. 2005

CONTENTS

THE ASEAN JOURNAL OF RADIOLOGY

Volume XI Number II MAY-AUG. 2005

CONTENTS

DOSE MEASUREMENT OF TOTAL SCALP RADIATION TREATMENT USING LATERAL PHOTON-ELECTRON TECHNIQUE

Chawalit LERTBUTSAYANUKUL[1] M.D., Chotika JUMPANGERN[1] M.Sc.
Chulee CHAROONSANTIKUL[1] M.Sc., Taweap SANGHANGTHUM[1] M.Sc.
Sivalee SURIYAPEE[1] M.Eng.

ABSTRACT

Purpose: To find the optimal abut or overlap area between photon-electron field and to measure superficial and intracranial dose using lateral photon-electron technique of total scalp radiation treatment.

Methods and Materials: CT scan of the Alderson Rando phantom was used in GE Target treatment planning system to find the optimal abut or overlap area between photon-electron fields. Each treatment fraction composed of two lateral-opposed fields of 6-MV photon (with square blocks) and two 9-MeV electron square fields. After the optimal plan was selected, film verification of the plan using solid water phantom instead of Alderson Rando phantom was performed. TLD chips were used to measure the intracranium and superficial skin dose of Alderson Rando phantom.

Results: Abutting photon-electron field resulted in 9-12 mm wide cold area along the junction. To compensate for this cold area, 6 to 7-mm overlapping between photon and electron irradiated field was applied in phase I of treatment and no overlapping photon-electron was used in phase II. This resulted in more homogeneous dose distribution. Film verification of the plan showed concordant result with the treatment planning system. By using TLD measurement, the average doses at frontal lobe, corpus collosum and parietal lobe relative to prescribed dose were 19.2, 12.3 and 10.9 %, respectively. The superficial skin doses at vertex and forehead relative to prescribed dose were 99 and 113.5 %, respectively.

Conclusion: Overlapping electron-photon field using square block in phase I and abutting electron-photon fields using square block in phase II were suggested as a useful technique to deliver homogeneous skin dose while avoiding the radiation dose to the underlying brain. The adaptability of the suggested photon block and electron insert has a great advantage and increases the convenience for clinical service. Since the distance between abutting and overlapping junction is very small, care must be taken in the setting up and the immobilization of the patient's head in the treatment room.

[1] Division of Radiation Oncology, Department of Radiology, King Chulalongkorn Memorial Hospital, Bangkok, Thailand

INTRODUCTION

Tumor of scalp is occasionally seen. It has many histological subtypes such as squamous cell carcinoma, angiosarcoma, melanoma and cutaneous lymphoma. Among these suptypes, angiosarcoma spreads transdermally for far wider than clinical appearance.[1] Surgical resection is unsuccessfully performed in such a widespread lesion. In this case, radiation therapy is the treatment of choice. The goal is to give a homogeneous dose distribution to the superficial scalp. This is quite difficult to achieve because of complex shape of the head. Moreover, the underlying brain should receive minimal radiation dose.

The lateral-opposed photon field with enough bolus is the simple technique which can provide adequate radiation dose to the scalp. Lead block is used to protect vital structures such as eyes. However, this technique irradiates too much of underlying normal brain.

A variety of radiotherapy techniques, including matching parallel-opposed photon and electron fields,[2,3] abutting electron fields,[4,5,6] and remote-controlled afterloading high-dose-rate (HDR) mold brachytherapy,[7,8] were suggested to overcome the inhomogeniety of dose. Yaparpalvi[6] proposed different energy electron beams as a simple alternative for achieving dose homogeniety. Also, intensity modulated radiation therapy (IMRT) has the potential for delivering homogeneous dose distribution to the scalp. However, Locke[9] reported that IMRT using tomotherapy resulted in a higher dose to the lens, brain, and orbit when compared to conventional lateral photon -electron technique. Electron arc or pseudoarc therapy used in breast irradiation[10,11] was not well established in scalp irradiation.

Because some techniques are complex and involve field matching problem, or may require sophisticated equipment such as IMRT; we then choose conventional parallel-opposed photon and electron fields proposed by Akazawa[2] and Tung[3] for treatment in our institution. Akazawa suggested no overlap area between photon and electron match line. While Tung suggested that electron field should overlap the photon field by approximately 3-4 millimeters to obtain more uniform dose distribution at the junction region. To alleviate the problem of overdose and under dose at the match line or overlap area, shifting of the junction was suggested. Both studies were performed in computer planning and in vivo measurement.

Regarding the different dose prescriptions, beam energy and set-up in our institution; we aimed to find the optimal abutting or overlapping edge which obtain a uniform dose distribution in the junction area and to use this technique as a class solution for irradiation of total scalp. The intracranial absorbed dose measurement was also reported.

MATERIAL AND METHOD

Since this is an experimental study and we would like to know the intracranial absorbed dose, The Alderson Rando® Phantom (The Phantom Laboratory, Salem, NY) was used to assess the in vivo dose distribution. Thermoplastic mask (MED TECH co.) was used to fix the phantom head in supine position.

Three-dimensional (3D) computed tomography of the Alderson Rando Phantom was obtained for treatment planning purpose. The treatment planning system is GE Target. To facilitate the set-up and ensure reproducibility; the 6-MV photon and 9-MeV electron fields, from Varian Clinac 1800, shared the same field center. A 100-cm source-to-surface (SSD) technique was implemented.

For the photon fields, fix-sized rectangular field (19x18 cm^2) was utilized. Fall-off at anterior, posterior and vertex of the head was confirmed for adequate skin flash. Caudal border was set up at the

bottom of C2 vertebral body. Square-shaped cerrobend blocks, 7.2x7.2, 8.4x8.4 and 9.8x9.8 cm^2, were made for photon shield at the center of the fields and must be symmetrical bilaterally. In the treatment planning system, these square-shaped cerrobend blocks were virtually created. For the electron fields, fix-sized square fields of 7.2x7.2, 8.4x8.4 and 9.8x9.8 cm^2 were created.

Each treatment fraction composed of two lateral-opposed fields of 6-MV photon and two 9-MeV electron fields. To avoid dose to the underlying brain, the photon fields were used to encompass median sagittal strip of the scalp while the electron fields irradiated central part of the lateral scalp as demonstrated in figure 1. Photon and electron doses were prescribed at the surface. The total dose of photon beam at surface was equal to the transit plus exit dose. Electron dose was then weighted and must be equal to total dose of photon beam. The prescription dose was 2 Gy per fraction. A 1.5-cm bolus was placed at each side of the scalp of Alderson Rando Phantom to bring the maximum dose to surface of the scalp. If the junction was shift, it would shift equally and divide the total dose into two phases.

Four types of the junctions were planned. First, non-overlap junction; photon block was equal to eletron field. Second, non-overlap junction with shifted junction; the same size of photon block and electron field was used in phase I and junction shift toward center of the field was used in phase II by reducing the size of photon block and electron field. Third, overlap junction; electron fields were larger than photon block. Fourth, overlap junction in phase I followed by non-overlap junction in phase II. A photon block which was smaller than the electron field was used in phase I, while a photon block which was equal to the electron field was used in phase II.

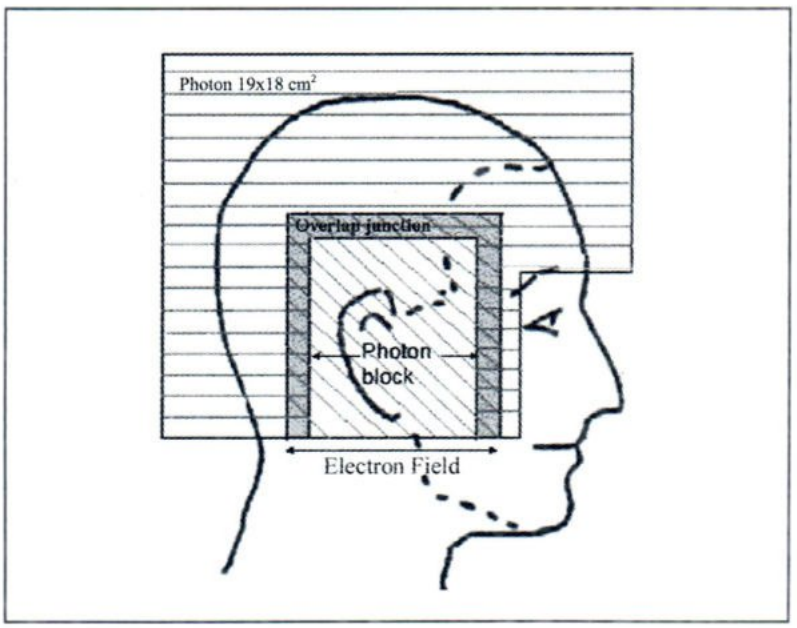

Fig.1 Shows the photon and electron fields irradiate to Alderson Rando Phantom. Horizontal line represents the photon fields while diagonal line represents electron field. Shade area represents the photon-electron overlap.

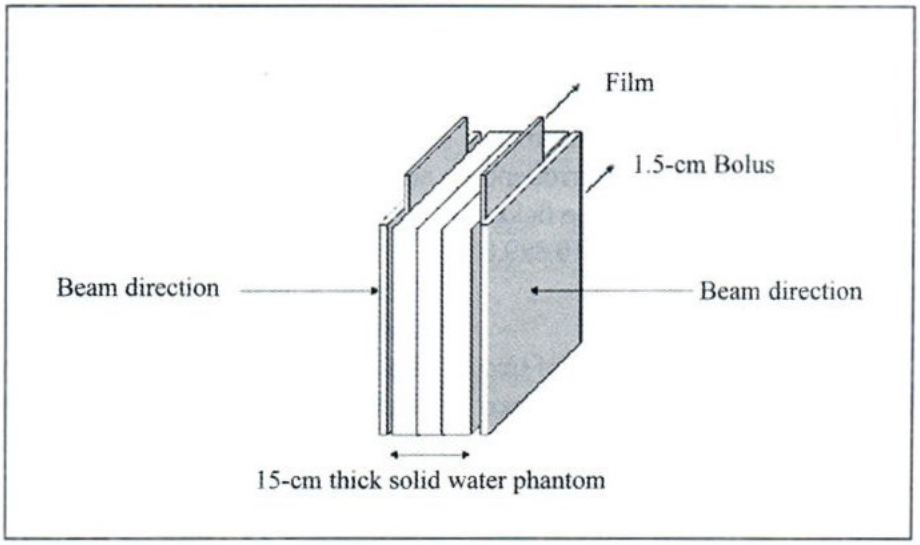

Fig.2 shows setting up solid water phantom for plan verification.

To verify the accuracy of treatment plan and to verify the hot and cold area; a solid water phantom with separation of 15 cm (same separation as Alderson Rando Phantom) was used for the treatment verification. The fields used in the treatment verification had the same geometry and accessories as their counterparts in the original Alderson Rando Phantom-planning plan. Kodak X-Omat V films were placed at both sides of solid water phantom. The films were then covered with 1.5-cm bolus bilaterally as shown in figure 2.

LiF TLD-100 chips were used to measure absolute dose on the skin surface and the intracranium of Alderson Rando Phantom. The existing regularly-spaced cavities in the intracranium of Alderson Rando phantom were used as measurement locations. At each measurement location, the absorb doses were read and averaged from the TLD chips. The linearity of TLD chips were calibrated for dose measurement between 150 and 300 cGy. To verify the stability of TLD chips, the standard group of TLD chips was irradiated with 100 cGy of 6-MV photon. Both the standard group and the study group TLD chips were read at the same time. The accuracy of the TLD dose measurements in this study was estimated to be ± 5 %

RESULTS

Using treatment planning system, we try to find the optimal overlap between photon and electron fields that gave the most homogeneous dose distribution (i.e., minimize the cold and hot area). The good junction composed of phase I and phase II altogether.

The acceptable range of uniform dose distribution at the junction in our experiment was 100 ± 10 % of the prescribed dose. Strip of cold and hot area beyond the acceptable range at the field junction was measured.

Table 1 demonstrates average cold area of non-overlap junction.

Experiment	Photon block (cm2)	Electron field (cm2)	Average cold area (mm)
No overlap 1	7.2x7.2	7.2x7.2	12
No overlap 2	9.8x9.8	9.8x9.8	9

Table 2 demonstrates average cold area of non-overlap junction with shifted junction

	Phase I		**Phase II**		**Cold Area**
experiment	Photon block (cm2)	Electron field (cm2)	Photon block (cm2)	Electron field (cm2)	Average (mm)
No overlap 1	8.4x8.4	8.4x8.4	7.2x7.2	7.2x7.2	12
No overlap 2	9.8x9.8	9.8x9.8	8.4x8.4	8.4x8.4	13.5

Non-overlap junction and no junction shift

Photon block and electron field at the same size were chosen (Table 1). This resulted in an abutment of photon and electron field. No junction shift was used. As expected, a cold area (i.e.,<90 % of the prescribed dose) of 9 to 12 mm wide along the field junction was observed.

Non-overlap junction with shifted junction

Subsequently, photon block and electron field at the same size were used at phase I. Junction shift toward center of the field was used in phase II by reducing the size of photon block and electron field (Table 2). Again, there was a cold area of 12 to 13.5 mm wide at the field junction.

Overlap junction

In this experiment, we tried to decrease cold area by making overlap between photon fields using 8.4x8.4 cm^2 square block and 9.8x9.8 cm^2 square electron field without junction shift (Table 3). Unfortunately, this process resulted in hot area for an average of 19 mm wide.

Table 3 demonstrates average hot area of overlap junction.

Experiment	Photon block (cm^2)	Electron field (cm^2)	Average hot area (mm)
overlap 7 mm	8.4x8.4	9.8x9.8	19

Table 4 demonstrates average cold or hot area when there was photon-electron overlap in phase I but no overlap in phase II

	Phase I	Phase II	Cold or hot		Area
Experiment	Photon block (cm^2)	Electron field (cm^2)	Photon block (cm^2)	Electron field (cm^2)	Average (mm)
Overlap 6 mm	7.2x7.2	8.4x8.4	8.4x8.4	8.4x8.4	0
Overlap 7 mm	8.4x8.4	9.8x9.8	9.8x9.8	9.8x9.8	0

Overlap junction and junction shift

In this experiment, we applied junction shift at the middle of treatment course. The overlap of photon-electron field was used in phase I. Nevertheless, there was no overlap of photon-electron field in phase II. This reduced the hot area and did not create any new cold area. The sizes of photon blocks and electron fields are shown in Table 4.

Film verification

According to the results of the above experiments (overlap 6 and 7 mm), film dosimetry was undertaken in the solid water phantom as described previously. Irradiated films were developed and scanned. Optical density was measured and interpreted. The relative dose at the field junction was concordant with the treatment planning result. Homogeneous dose distribution along field junction was observed.

Absolute dose measurement

Optimal plans from table 4 were used for irradiation of the Alderson Rando phantom. TLD chips were placed in the intracranium of the phantom. The TLD chips measured the absorbed dose in the position representing frontal lobe, corpus collosum, parietal lobe, occipital lobe and cerebellum. The absorbed doses were normalized to prescribed dose. The average doses at frontal lobe, corpus collosum and parietal lobe were 19.2, 12.3 and 10.9 %, respectively. These areas were under the photon block. Doses at occipital lobe and cerebellum were 74.3 and 96.5 %, respectively. These areas absorbed the dose from the photon fields (parasagittal region).

TLD chips were also placed at the skin surface at vertex and forehead. The corresponding doses were 99 and 113.5 %, respectively. These areas received dose exclusively from bilateral opposed photon field.

DISCUSSION

Total scalp irradiation is a challenging procedure because of complex shape of the head. Various treatment techniques were suggested to ensure dose uniformity along scalp while minimizing dose to the underneath brain. Abutting electron field technique,[4,5,6] electron arc therapy,[10,11] mould brachytherapy[7,8] and IMRT[9] are labor intensive and require sophisticated equipment. The current study proved that even simple technique using bilateral opposed photon-electron matching beams can produce dose homogeneity. This technique required a wax bolus placing over the scalp in order to bring the dose to the skin. Field shifting is usually applied to minimize hot spot.

The drawback of this technique is that it requires the accuracy on the process of cut block, making photon shield and daily setup. Moreover, the treatment was divided into 2 phases by shifting the

overlap junction. The overlap of photon-electron field in phase I resulted in hot spot in the junction area while the non-overlap of photon-electron field in phase II resulted in cold spot in the same area. Thus, the biological effect on the junction would not be uniform on the daily basis. To minimize the non-uniform dose based on biological effective dose, two-phase treatment on the same day (i.e., prescribed 1 Gy from phase I and 1 Gy from phase II) would result in more biologically uniform dose. However, trade off between the setup time and the biological effective dose should be considered. An alternative way is to deliver the dose in phase I and II on alternate day fashion.

The optimal overlap of photon-electron field in our study is 6 mm. This figure was different from 3.5 ± 1 mm reported by Tung.[3] However, Locke[9] discovered that an additional margin of overlap was required over the posterior vertex area. The difference could be explained by the disagreement of the electron energy from different machine, technique and different bolus thickness among the studies.

Tung[3] reported that 10% of the brain received dose more than 45 Gy (prescribed dose = 55 Gy). While Locke[9] reported 20% of brain received dose more than 20 Gy (prescribed dose = 50.4 Gy). In this study, although, we did not calculate the dose volume histogram, but our result showed that high dose region was limited to the area irradiated exclusively by bilateral photon fields. The dose to the brain depends on size of the photon block; the larger the photon block, the less dose to the brain.

Making photon blocks and electron metalloid inserts requires experience. A 3-4 mm difference in width of the round-shape block is hardly met. This meant that the block itself would be even very small difference in size and prone to setup error. Our solution was to make a 6-7 mm difference in width of the blocks and electron inserts between phase I and II. Three square photon shields at 7.2x7.2, 8.4x8.4 and 9.8x9.8 cm^2, and three electron inserts at 7.2x7.2, 8.4x8.4 and 9.8x9.8 cm^2 are recommended to be used in clinical service. Matching of photon block and electron inserts was chosen based on sizes of the patients' heads. Special care must be given for radiation therapist in setting up and immobilizing patients' heads in the treatment room so as to decrease random error along the field junction.

CONCLUSION

Total scalp irradiation is a rare indication in clinical service. Abutting electron-photon fields using square block was suggested as a useful technique to deliver homogeneous skin dose while avoiding dose to underlying brain. The adaptability of the suggested photon block and electron insert has a great advantage and increases the convenience for clinical service.

ACKNOWLEDGEMENTS

The authors would like to express our sincere thanks to the Vej Dusit Foundation who gived financial support of this project.

REFERENCES

1. Rosai J, Sumner HW, Major MC, et al. Angiosarcoma of the skin. Hum Patho 1976; 7(1): 83-109
2. Akazawa C. Treatment of the scalp using photon and electron beams. Med Dosi 1989; 14(2):129-131
3. Tung SS, Shiu AS, Starkschall G, Morrison WH, Hogstrom KR. Dosimetric evaluation of total scalp irradiation using a lateral electron-photon technique. Int J Radiat Oncol Biol Phys 1993 Sep; 27(1):153-160
4. Able CM, Mills MD, McNeese MD, Hogstrom KR. Evaluation of a total scalp electron irradiation technique. Int J Radiat Oncol Biol Phys 1991 Sep;21(4):1063-1072
5. McKenzie AL. A simple method for matching electron beams in radiotherapy. Phys Med Biol 1998 Dec;43(12):3465-3478

6. Yaparpalvi R, Fontenla DP, Beitler JJ. Improved dose homogeneity in scalp irradiation using a single set-up point and different energy electron beams. Br J Radiol 2002 Aug;75(896): 670-677
7. Ozyar E, Gurdalli S. Mold brachytherapy can be an optional technique for total scalp irradiation. Int J Radiat Oncol Biol Phys 2002 Nov; 54(4):1286-1288
8. Nakamura R, Harada S, Obara T, Ehara S, Yoshida A, Akasaka T, et al. Iridium-192 brachytherapy for hemorrhagic angiosarcoma of the scalp: a case report. Jpn J Clin Oncol 2003 Apr; 33(4):198-201
9. Locke J, Low DA, Grigireit T, et al. Potential of tomotherapy for total scalp treatment. Int J Radiat Oncol Biol Phys 2002 Feb; 52(2): 553-559
10. McKenzie MR, Freeman CR, Pla M, Guerra J, Souhami L, Pla C, et al. Clinical experience with electron pseudoarc therapy. Br J Radio 1993 Mar, 66:234-340
11. Leavitt DD, Peacock LM, Gibbs FA, et al. Electron arc therapy: physical measurement and treatment planning techniques. Int J Radiat Oncol Biol Phys 1985; 5:987-995

PULMONARY FINDINGS OF AVIAN INFLUENZA A (H5N1) PNEUMONIA OF A FAMILY CLUSTER IN KAMPHAENGPHET OUTBREAK.

Chanya CHAISIRIRAT M.D.[1]

ABSTRACT

Until now, avian influenza pneumonia is very hot issue and life threatening disease in Kamphaengphet, in Thailand and in Asian countries. Recent outbreak of avian influenza A (H5N1) in rural areas of Kamphaengphet Province and human infection with this virus were occurred in September 2004 (second outbreak in Thailand).

The object of this report was to show the epidemiology, clinical features and pattern of pulmonary findings that could be found in avian influenza pneumonia, which might be helpful for future diagnosis and comparison of this disease with the next outbreaks.

We reviewed the pulmonary findings of a family cluster of three involved patients. Two confirmed cases were mother and aunt. They have been confirmed as cause by H5N1 strain by viral study. The mother was dead but the aunt has been survived. One probable case was the index girl. She was the first fatal case and was under investigation for H5N1 on admission due to initial diagnosis was dengue hemorrhagic shock syndrome. However, her retrospective diagnosis was presumed by a history of exposure to infected household chickens, and clinical features that corresponding to cardinal features of previously reported cases, and her mother's death from severe H5N1 pneumonia after having close contact with her.

In fact, the mother had no history of exposure to poultry, so we believe that the avian influenza H5N1 virus was probably transmitted directly from the infected girl to the mother after unprotected bedside care. No additional cases were identified among contacts.

The radiographs of these three involved patients were abnormal on admission. All pulmonary findings were air space patterns, including unilateral and bilateral lesions, patchy infiltration and lobar consolidations.

INTRODUCTION

Avian influenza is an infected disease of birds, cause by type A strain of the influenza virus. The disease which was first identified in Italy more than 100 years ago and had been occurred worldwide with some influenza virus subtypes.[1] First documented avian influenza (H5N1) infection of human occurred in Hong Kong in 1997. The 1997 outbreak of influenza A (H5N1) in Hong Kong established that highly pathogenic avian influenza viruses can infected human directly with resulting in severe respiratory illness that was fatal in 6 of 18 patients.[1,2,3,4,5,6] This outbreak ended abruptly after the culling of poultry.[1]

[1] Department of Radiology, Kamphaengphet Hospital, Kamphaengphet 62000, Thailand

However the later current outbreaks presented challenges because of the large geographic areas and large numbers of affected poultry.[7]

In late 2003 and early 2004, there were reports of large outbreaks of highly pathogenic avian influenza A (H5N1) and more widespread among poultry farms in Asian countries-Cambodia, Indonesia, Japan, Laos, South Korea, China, Vietnam and Thailand.[3,5,6,7] Direct infection of human with H5N1 related to these poultry outbreaks (avian to human spread) were confirmed in Thailand and Vietnam.[3,5,8] As of November 11, 2004, H5N1 infected at least 44 human cases, of which 32 were fatal.[4,8,9]

First outbreaks in Thailand in early 2004, the disease were found in a community of chicken farms in Ayuthaya and Pathum Thani Provinces. The causative agent was identified as H5N1 influenza virus. Human cases were recognized in Sukhothai, Kanchanaburi and Suphan Buri Provinces.[10,17,18]

H5N1 avian influenza usually has limited capacity to infect humans because of host barrier to infection. However, the H5N1 infected human cases were confirmed and reported at least five occasions since 1997.[7] In most of the human cases were thought to have resulted from exposure to infected poultry and the man to man transmission has not been clearly detected.[10] But to date, there have been several recent studies of possible limited person to person transmission. Such event occurred in 1997 in Hong Kong, two health care workers who had taken care of the patients were later found to have antibodies to hemagglutinin H5N1 and one developed respiratory illness.[3,4,8,15] Two family clusters in Vietnam in 2004 were also considered to be compatible with possible limited person to person transmission.[3,6,12]

The reported symptoms of avian influenza infection in humans have ranged from asymptomatic infection to typical influenza-like symptoms (e.g., fever, cough, sore throat, and muscle aches), conjunctivitis, fatal pneumonitis, acute respiratory distress, other life-threatening complications and multiple organ failure. Lymphopenia, thrombocytopenia and positive chest radiographs were observed among patient with severe infection.[2,3,5,6,7,8,9,13,14,16,17,18]

CASE REPORTS

Patient 1

The patient 1 was a first fatal case in Kamphaengphet Province and was under investigation for avian influenza H5N1 infection.

A 11 year old girl (index case) who lived with her aunt in area with abnormal poultry deaths in the village of Kamphaengphet Province. She had significant history of exposure to sick and dying household chickens for 3-4 days before the onset of illness. She presented to a clinic with symptoms of fever, cough, sore throat and dyspnea on September 2, 2004. Few days later she was admitted to the District Hospital with progressive respiratory illness on September 7, 2004. The initial diagnosis was dengue hemorrhagic fever. Because of progressive worsening, she was transferred to pediatric department of Kamphaengphet Hospital on September 8, 2004 (day 7 of her illness). She developed progressive respiratory distress, hypoxia and shock, leading to rapid dead for only three hours later after admission in spite of aggressive support, including intubation and mechanical ventilation, broad-spectrum antibiotics and fluid resuscitation. Initial diagnosis was dengue shock syndrome, pneumonia or septicemia.

A serum sample was negative for antibody to dengue virus and inadequate residual serum sample to test for hemaglutinin H5.

Chest radiography revealed right lower lobe consolidation and left lower lobe patchy infiltration (Fig. 1A-B)

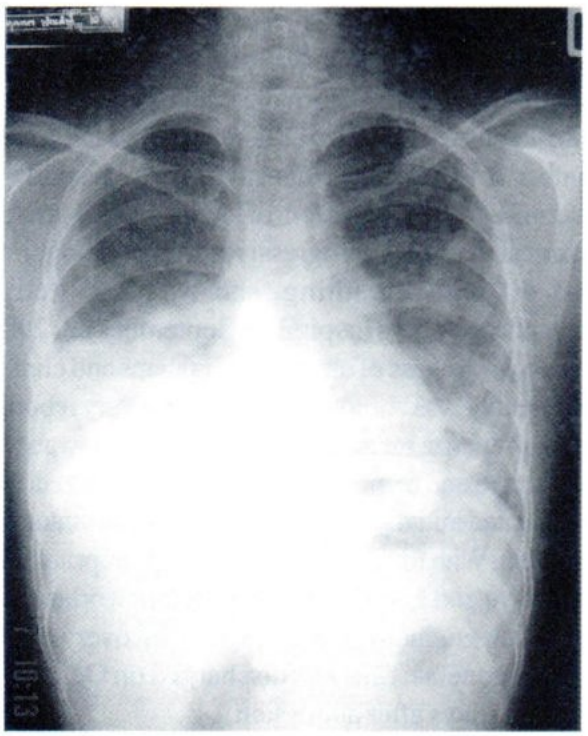

Fig.1A On day 6

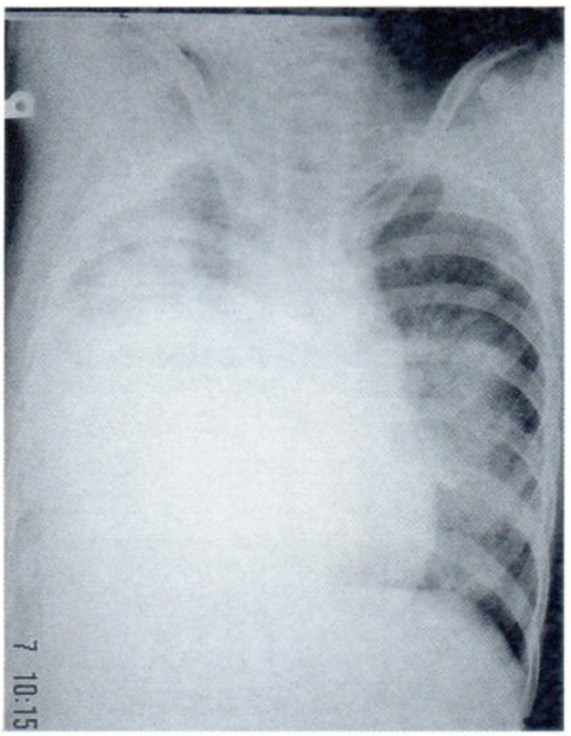

Fig.1B 9 hours later

Fig.1A-B Chest radiographs of patient 1 (index girl) on day 6 of her illness, revealed rapid progressive right lower lobe consolidation with left lower lobe patchy infiltration and air bronchogram. AP view (Fig.1A), 9 hours later (Fig.1B)

Patient 2

The index girl's mother was 26-year-old woman, who lived in Nonthaburi Province. She came to visit and provided unprotected bedside care for her hospitalized daughter (patient 1) during the last 2 days of her daughter's life, before the girl died. She sat on the bed, wiped secretions, hugged and kissed her daughter all the times. She developed flu-like symptoms three days later on September 11, 2004, and still stayed in her daughter's village for one night and returning to her home in the following morning.

On September 17, 2004, she was admitted to her own provincial hospital with severe pneumonia and progressive respiratory failure. She died on September 20, 2004.

Testing for hemaglutinin H5 was positive for reverse transcriptase polymerase chain reaction (RT -PCR) of autopsy lung tissue.

Chest radiography revealed bilateral lower lobe consolidations.[8] (Fig. 2)

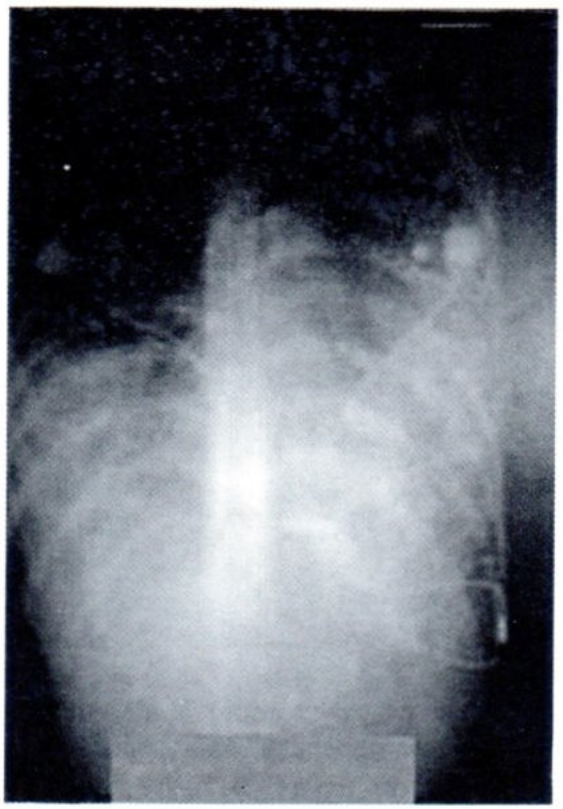

Fig.2 Chest radiograph of patient 2 (index girl's mother) on day 9 of her illness, revealed bilateral lower lobe consolidations and air bronchogram.[8]

Patient 3

A 32 year old index girl's aunt lived with her niece (patient 1). She provided unprotected bedside care on day 6 of her niece's illness. 9 days later (September 16, 2004), she began the onset of respiratory tract infection with symptom of fever, myalgia and chill. According to rapid progressive severe pneumonitis and difficult breathing, she was admitted to Kamphaengphet Hospital on September 23, 2004. Due to awareness of attending clinicians and clinical feature that was compatible with previously reported avian influenza infection, so oropharyngeal swab was performed and respiratory specimens was tested. She was treated initially with oseltamivir and instituted full isolation. With rapid diagnosis, earlier prompt antiviral treatment and good team of health care workers, her condition gradually improved, fully recovery and no major sequelae. She was discharged on October 7, 2004, 14 days after admission.

Testing for hemaglutinin H5 was positive for reverse transcriptase polymerase chain reaction (RT -PCR) of oropharyngeal swab. Culture of respiratory and blood specimens did not show bacterial pathogens.

Chest radiography revealed left lower lobe consolidation. (Fig. 3 A-H)

Table1 Clinical Features of the Family Cluster of Avian Influenza (H5N1)

Patient	Age (yr)	Date of onset	Date of admission	Chest Radiograph	Antiviral treatment	Respiratory Isolation	Viral study	Outcome
Girl	11	Sept. 2	Sept. 7	Bilateral lower-lobe consolidation	No	No	Inadequate sample	Died Sept. 8
Mother	26	Sept. 11	Sept. 17	Bilateral lower-lobe consolidation	No	No	Positive (RT-PCR of lung tissue)	Died Sept. 20
Aunt	32	Sept. 16	Sept. 23	Left lower-lobe consolidation	Yes	Yes	Positive (RT-PCR of oropharyngeal swab)	Survived; discharged Oct. 7

Source: Adapted from Unchusak K. et al., 2005.[8]

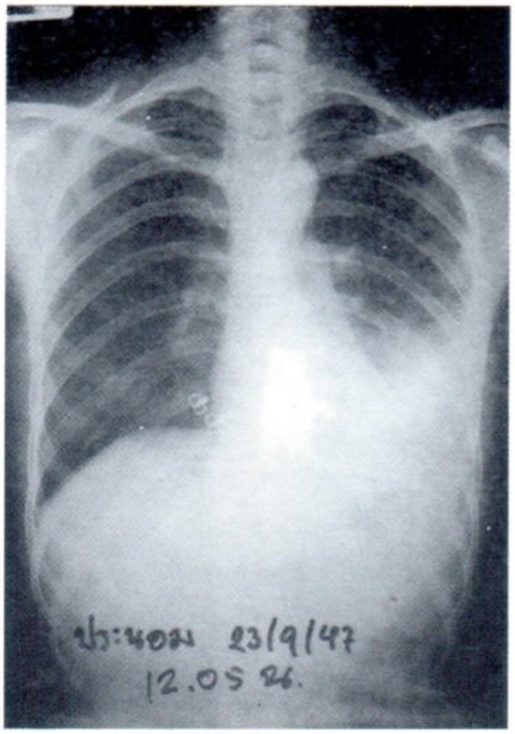

Fig.3A On admission, Sep. 23, 2004

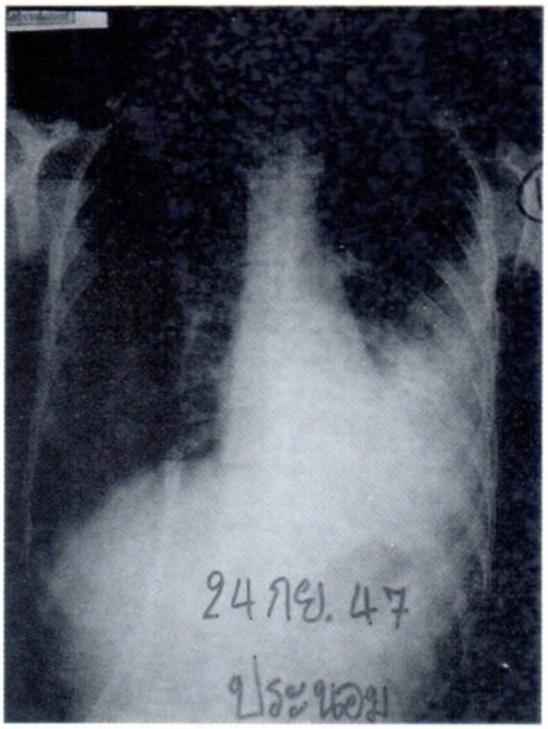

Fig.3B On day 2, Sep. 24, 2004

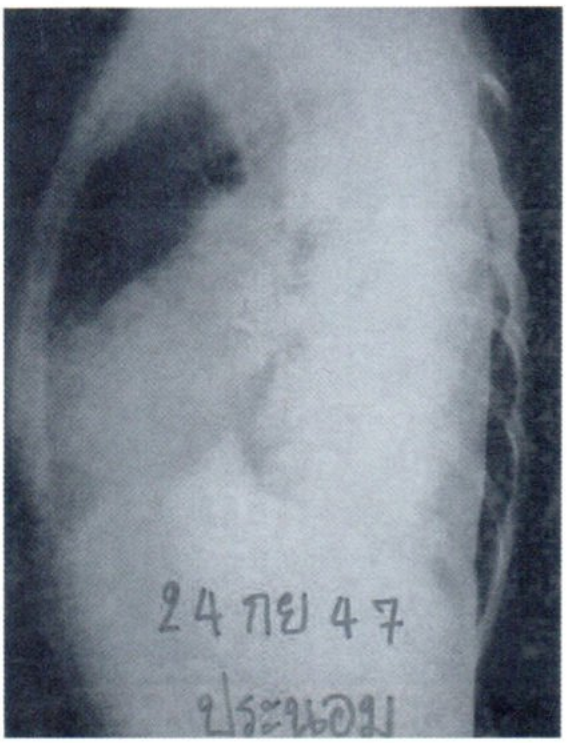

Fig.3C On day 2, Sep. 24, 2004

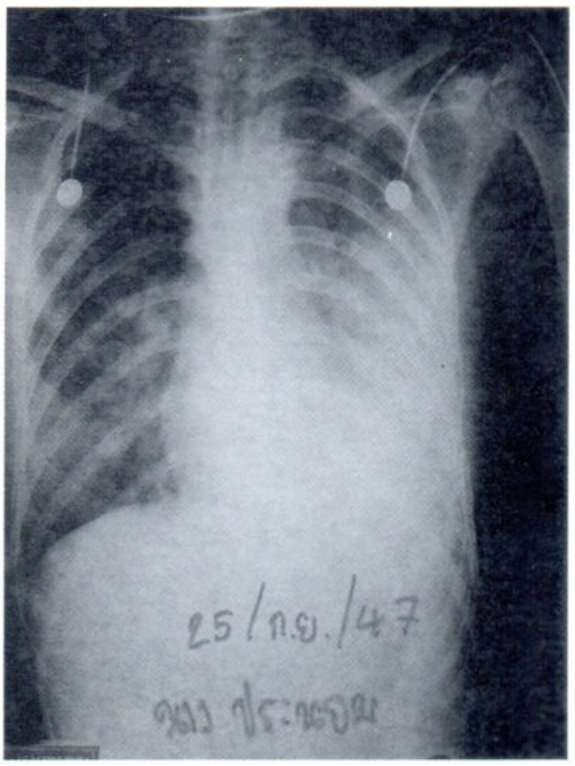

Fig.3D On day 3, Sep. 25, 2004

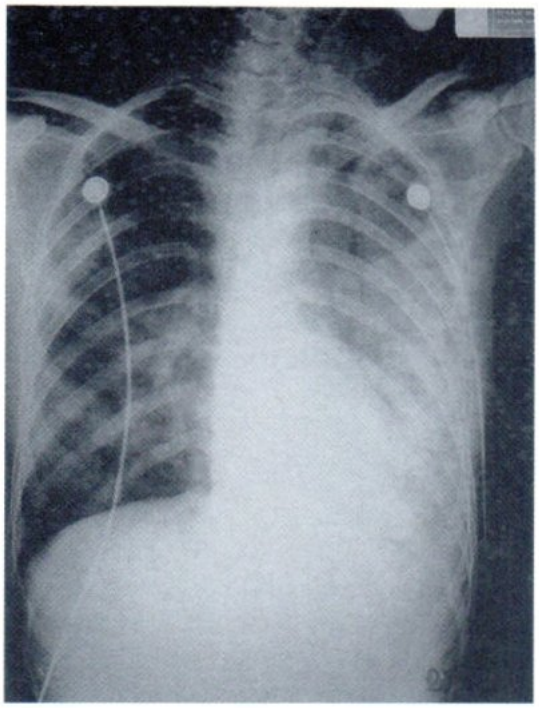

Fig.3E On day 5, Sep. 27, 2004

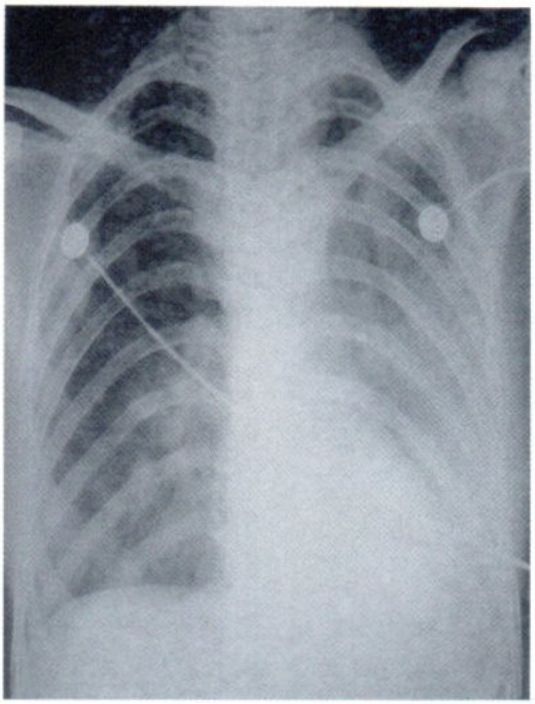

Fig.3F On day 7, Sep. 29, 2004

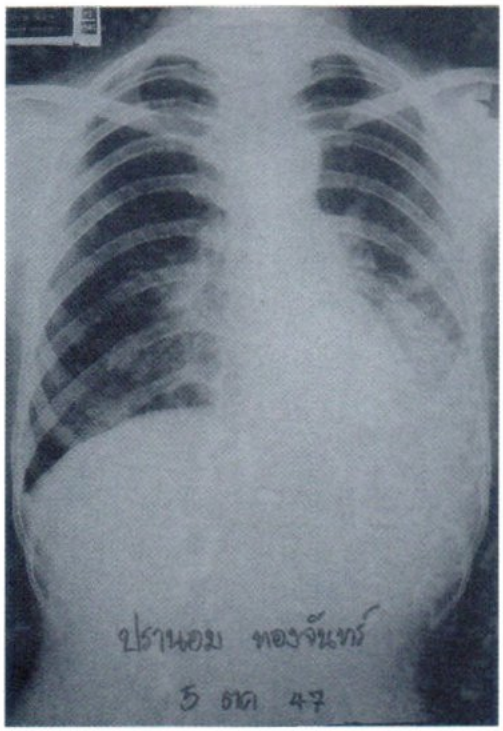

Fig.3G On day 13, Oct. 5, 2004

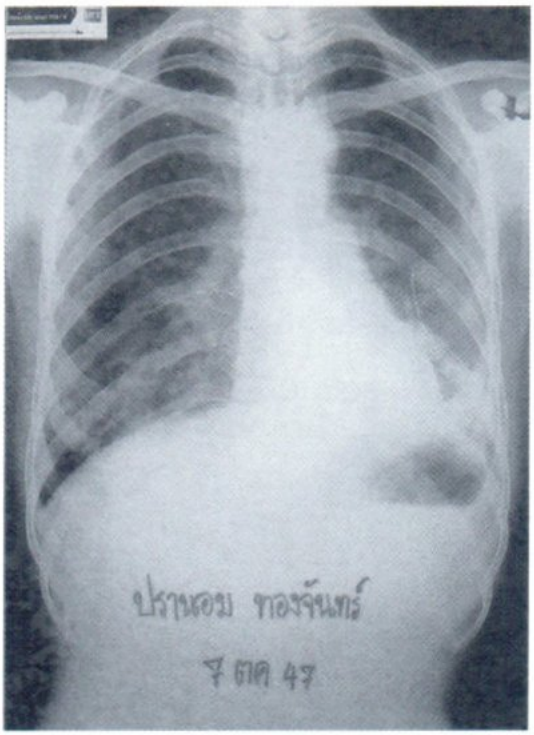

Fig.3H On discharge, Oct. 7, 2004

Fig.3 A-H Serial chest radiographs of patient 3 (index girl's aunt) demonstrated left lower lobe consolidation with gradual improvement and nearly complete clearing on the day of discharge.

DISCUSSION

In Kamphaengphet Hospital, since September 8 to November 22, 2004, there were 72 patients who presented with influenza like illness and pneumonia, and had history of poultry exposure or lived in areas of abnormal poultry death. There were one probable index case and two confirmed cases.

All of our three patients presented with influenza like symptoms, severe respiratory illness, lymphopenia and abnormal chest radiographs on admission that corresponding with signs and symptoms of previously reported human cases.

The diagnosis of the index girl (patient 1) could not be confirmed by viral study, but to be presumed by (1) history of exposure to infected household chickens, (2) clinical features of influenza like symptoms and fatal pneumonitis, correspond to the cardinal features of previously reported human cases. And (3) the death from H5N1 avian flu pneumonia of the mother despite of absence poultry exposure, 12 days after her daughter died of the disease, has raised support that this virus also cause the disease in the girl.

The mother and aunt had no exposure to poultry within the accepted incubation period (2-10 days). So we believe that the disease in the mother and aunt probably resulted from human to human transmission during the prolonged face-to-face unprotected bedside care for the infected girl.[3,8,14] However, it was limited within a family. No other household members, other family contacts, exposed neighbors or exposed health care workers were later found to be ill within14 days, but still continued closed active surveillance.[8,14]

Only the aunt has been survived, due to awareness, rapid diagnosis and earlier prompt antiviral treatment. Early detection and appropriated management of the illness are essential, since treatment with antiviral agents is likely to be beneficial only when it is started early in the course of the illness.[16]

We classified chest radiograph findings as normal, interstitial infiltration and air space pattern by using standard criteria. The pulmonary findings of our three involved patients were air space patterns with unilateral and bilateral lobar consolidations, mimic usual features of bacterial pneumonia.

Our study has been supported by several previous studies in Hong Kong, Thailand and Vietnam. At the beginning of 2004, clinical features of 5 Thai fatal confirmed cases and 10 Vietnamese cases have been reported.[6,7,17,18] All Thai patient had apparent pneumonia progressing to respiratory failure. Their chest radiograph changes were observed with patchy infiltration in four and interstitial infiltration in one.[17,18] Chest radiographs of 10 Vietnamese infected avian influenza pneumonia were reviewed by Tran Tinh Hien et al., the radiographic findings were categorized with attention to unilateral or bilateral changes, focal, lobar and patchy consolidations, air space infiltrates, air bronchogram, similar findings of our report.[6]

12 confirmed cases from January to March 2004 in Thailand were reported by Chotpitayasunondh T. Et al. Two patients had interstitial infiltration and 10 patients had patchy lobar infiltration in a variety patterns (single lobe, multiple lobes, unilateral or bilateral distributions).[5]

A family cluster in Hong Kong in the beginning of 2003, infected boy and his father had characteristic respiratory illness of avian influenza pneumonia, and chest radiographs appear to have left lingular lobe consolidation and right lower lobe consolidation, respectively.[11]

According to few infected human cases were collected since the large outbreaks in Hong Kong in 1997, and limited information about pulmonary finding details, so unable to specify the characteristic pulmonary findings of avian influenza pneumonia.

However, almost of our reviewed cases were air space pattern. We hope that our report may be helpful for future diagnosis, in comparison with findings to another and next outbreaks, finally initiate the investigation team to concern and learn about patterns of pulmonary features.

De Jong MD et al. report an additional a Vietnamese family cluster of two fatal confirmed cases who presented with atypical symptoms by severe diarrhea followed by rapid progressive coma, convulsion and acute encephalitis but no apparent of respiratory illness and primarily negative chest x-ray findings, suggested that the clinical spectrum of influenza H5N1 is wider than previously thought and clinical surveillance should focus not only on respiratory illness but also on clusters of unexplained deaths or severe illness of any kind.[12,16]

CONCLUSION

Avian influenza is an infected disease of birds and poultry.

Directed infection of human has been clearly confirmed but not often in frequency, carrying a high risk of death.

Clinical experience with avian H5N1 disease in human is limited. However certain helpful features are, direct exposure to ill poultry with flu-like symptoms, progressive respiratory illness, lymphopenia and abnormal chest radiographs.

The majority of abnormal chest radiographs were air space patterns.

Atypical symptoms without primarily respiratory illness were reported in Vietnam.

Sustained human to human transmission of H5N1 has not yet been confirmed. However, influenza viruses are genetically variable and transmissibility is difficult to be predicted. Therefore, the health care workers and the contacts should continue to take measures to protect themselves with the assumption that, human to human transmission can occur.

Due to increasing evidence of infected human cases, progressive more virulence and high mortality, so clinicians must remain alert and continued monitoring about the disease.

Good preparation for future outbreaks, early detection in order to initiate optimal antiviral therapy, information shared and infection-control measures for both animal and humans are very important.

ACKNOWLEDGEMENT

I am indebted to Dr. Kamchai Rangsimunpaiboon, the chief of Kamphaengphet Provincial Hospital, for his supports during the preparation, Dr. Angkana Upapong and Dr. Rotjana Khontong, attending clinicians who gave me the patient's details and reference papers.

I would like to thank the Infectious Control Committee of Kamphaengphet Hospital for patient's profiles.

REFFERENCES

1. World Health Organization. Avian influenza ("bird flu") and the significant of its transmission to humans. Avian influenza - fact sheet, January 15, 2004.
2. Chan PK. Outbreak of avian influenza A (H5N1) virus infection in Hong Kong, 1997. Clin Infect Dis 2002; 34:S58-64.
3. Liem NT et al. Lack of H5N1 avian influenza transmission to hospital employees, Hanoi, 2004 Emerg Infect Dis 2005 Feb;11:210-5.
4. Monto AS. The threat of an avian influenza pandemic. N Engl J Med 2005; 352:323-325.
5. Chotpitayasunondh T et al. Human disease from influenza A (H5N1), Thailand 2004. Emerg Infect Dis 2005 Feb; 11:210-5.

6. Hien TT, Liem NT, Dung NT et al. Avian influenza A (H5N1) in 10 patients in Vietnam. N Engl J Med 2004; 350:1179-88.
7. CDC. Outbreaks of avian influenza A (H5N1) in Asia and interim recommendations for evaluation and reporting of suspected case -United state, 2004. MMWR Morb Mortal Wkly Rep 2004; 53:97-100.
8. Unchusak K. et al. Propably Person-to-Person Transmission of Avian Influenza A (H5N1). N Engl J Med 2005 Jan 27; 352:333-340.
9. Storhr K. Avian influenza and pandemics -Research needs and opportunisties. N Engl J Med 2005 Jan 27; 352:405-407.
10. Thailand Minister of Public Health. Note on avian influenza situation, July 12, 2004. Available from.
11. ProMed-mail. Influenza A (H5N1) in Hong Kong Special Administrative Region of China-Update. http.//www.promedmail.org; 20 Feb 2003.
12. Jane Parry. Official report first Cambodian case of avian flu. BMJ 2005;330:273 (5 February) doi:10.1136/bmj.330.7486. 273 news.
13. (2005) Avian influenza: high mortality but inefficiency person to person spread - So Far. Journal Watch.
14. Thailand Ministry of Public Health. Press Release: Avian influenza infectious of patients in Kamphaenphet (Sep 28, 2004) (accessed 2004 October 11). Available from.
15. Bridges CB, Katz JM, Seto WH, et al. Risk of influenza A (H5N1) infection among health care workers exposed to patient with influenza A (H5N1), Hong Kong. J Infect Dis 2000; 181:344-8.
16. De Jong MD et al. Fatal avian influenza A (H5N1) in a child presenting with diarrhea followed by coma. N Engl J Med 2005 Feb 17; 352:686-91.
17. CDC. Cases of influenza A (H5N1) - Thailand, 2004. MMWR Morb Mortal Wkly Rep 2004; 53:100-3.
18. Thailand Ministry of Public Health.Preliminary clinical description of influenza A (H5N1) in Thailand Available from http://www.epid. moph. go.th./weekly/WESR 47/GROUP2/group_2 _30.html

SURVIVAL ANALYSIS OF STAGE I-IIIA BREAST CANCER PATIENTS TREATED WITH MASTECTOMY; 11-YEAR EXPERIENCE IN KING CHULALONGKORN MEMORIAL HOSPITAL

Chawalit LERTBUTSAYANUKUL M.D.,[1] Prasert LERTSANGUANSINCHAI M.D.[1]
Kanjana SHOTELERSUK M.D.,[1] Chonlakiet KHORPRASERT M.D.,[1]
Sivalee SURIYAPEE M.Eng,[1] Chesada SANGSUBHAN M.D.,[2]
Patpong NAVICHARERN[2]

ABSTRACT

A retrospective review was performed on 357 stage I-IIIA breast cancer patients who were treated with mastectomy and had been referred to radiation oncology unit, King Chulalongkorn Memorial Hospital, between January 1991 and December 2001. The primary objectives were to report the overall survival and relapse-free survival rates. Survival rates were also stratified by stages, tumor sizes, number of positive axillary lymph nodes and the effect of adjuvant treatment.

The median age in the present study was 49 years. The number of patients were 39, 132, 152 and 34 in stage I, II A, II B and III A respectively. Adjuvant Chemotherapy was given to 247 patients (69.2 %), while adjuvant hormonal therapy was given to 122 patients (34.2 %). Sixty one patients (17.1 %) received both adjuvant chemotherapy and hormonal therapy. Median follow up time was 42.6 months (range 6-136 months).

Five-year overall survival and relapse-free survival rates for the whole group were 72.3% and 58.6%, respectively. The 5-year overall survival rates were 75.2%, 81.0%, 69.0% and 49.8% for stage I, IIA, IIB and IIIA, respectively (P= 0.0001). The corresponding 5-year relapse-free survival rates were 53.9%, 68.1%, 57.5%, and 32.1%, respectively (P = 0.0017). Factors significantly affect overall survival rate composed of stages, T-stage, number of positive lymph nodes and regimens of chemotherapy.

Overall, our results of breast cancer treatment in King Chulalongkorn Memorial Hospital were comparable to the previous reports in medical literatures. This study provided base line data of breast cancer treatment results in Thailand, King Chulalongkorn Memorial Hospital.

Key words: Breast cancer, mastectomy, Stage I-IIIA, Survival analysis

[1] Division of Radiation Therapy, Department of Radiology, Faculty of Medicine, Chulalongkorn University, Bangkok, Thailand
[2] Department of Surgery, Faculty of Medicine, Chulalongkorn University, Bangkok, Thailand
Correspondence: Chawalit Lertbutsayanukul M.D.
Division of Radiation Therapy, Department of Radiology, Faculty of Medicine, Chulalongkorn University
1873 Rama IV Road, Patumwan, Bangkok, Thailand 10330

INTRODUCTION

Breast cancer has become a major impact on the health problem of Thai women. For several decades, there had been a dramatic increase in the incidence of invasive breast cancer. The estimated incidence rate was increased from 16.3 in 1994 to 7.2 in 1997 per 100,000.[1,2] In 2000, there were 307 new breast cancer patients treated in King Chulalongkorn Memorial Hospital.[3] This figure increased to 374 in 2001.[4] There was also an increase of new breast cancer patients in Siriraj Hospital.[5]

Surgery is the main treatment for early breast cancer patients. However, postoperative adjuvant therapy is considered an essential part of the management of early breast cancer. Adjuvant chemotherapy typically produces an absolute improvement of about 7-11% in 10-year survival for women aged under 50 with early breast cancer, and of about 2-3% for those aged 50-69.[6] Similarly, adjuvant tamoxifen treatment substantially improves the 10-year survival of women with positive-estrogen-receptor (ER) tumors and of women whose tumors are of unknown ER status.[7]

Since there is a trend that breast cancer incidence will be the first leading cancer in Thai women and the lack of a large-scaled published data in Thai population, we retrospectively studied our patients as base line data for future comparison. The primary end points were overall survival and relapse -free survival rates. Survival rates were also stratified by stages, tumor sizes, number of positive axillary lymph nodes and the effect of adjuvant treatments.

MATERIAL AND METHOD

Patients

All records of patients with stage I-IIIA operable breast cancer who underwent mastectomy between Jan 1991 to Dec 2001 were retrospectively reviewed. The diagnosis of breast cancer was confirmed histopathologically. Modified radical mastectomy was performed with level I and II axillary lymph node dissection. Patients with concurrent distant metastasis or previous diagnosis of other cancer were excluded. Neoadjuvant chemotherapy or preoperative irradiation was not eligible. There were 371 patients in this review but only 357 patients were analyzed. Fourteen patients were ineligible; 7 patients refused adjuvant therapy, 4 patients were referred to other hospitals and 3 patients presented with distant organ involvement after metastases work up. Hormonal study, estrogen (ER) and progesterone (PgR) receptors, was evaluated by immunohistochemistry.

Treatment

Since this is a retrospective review, there were mixed groups of adjuvant treatment. Our policy of adjuvant treatment between the reviewed period is summarized in table 1. The details of radiation therapy technique have been reported.[8] Systemic adjuvant chemotherapy was used in high-risk patients. The regimens were CMF (Cyclophosphamide 600 mg/m^2, Methotrexate 40 mg/m^2 and 5 Fluorouracil (5 FU) 600 mg/m^2 intravenous every three weeks) and FEC (Cyclophosphamide 600 mg/m^2, Epirubicin 60 mg/m^2 and 5FU 600 mg/m^2 intravenous every three weeks) for six cycles. Regarding hormonal therapy, Tamoxifen 20 mg/day was usually prescribed for patients with positive estrogen (ER) and/or progesterone (PgR) receptor. Tamoxifen was given for 5 years and started after completion of adjuvant chemotherapy and/or radiation therapy.

Statistical analysis

Overall survival rate was calculated from the date of surgery to death. Data on patients who were alive or lost to follow-up were censored on the date of last follow-up. Relapse-free survival rate was calculated from the date of surgery to the date of local, regional or distant metastases. Overall survival

and relapse-free survival rates were calculated by the Kaplan-Meier method[9] and differences between groups were compared by the log-rank test.[10] Subgroup analyses were stratified by stage grouping, T-stage, number of lymph node metastasis and adjuvant treatment. The AJCC 1997 cancer staging system was used in this study.[11]

RESULTS

Patient characteristics is demonstrated in table 2. Median follow-up time was 42.6 months (range 6-136 months). T1, T2 and T3 tumors were found in 20.2%, 66.9% and 12.9% of the patients, respectively. Regarding nodal status, 43.7% were negative axillary lymph node whereas 56.3% were positive axillary lymph nodes. According to AJCC 1997 stage grouping, there were 10.9%, 37.0%, 42.6% and 9.5% of patients in stage I, IIA, IIB and IIIA, respectively. The correlation between T stage and number of positive axillary lymph nodes is shown in table 3. The median age in the present study was 49 years.

The adjuvant therapy in the present study is shown in table 4. Adjuvant radiation therapy was given to 55.2% (197/357) of all patients, whereas adjuvant chemotherapy was given to 69.2% of the patients. Of those who received chemotherapy, CMF regimen was used in 61.1% while anthracycline-based regimen was used in 35.2%.

Regarding hormonal receptor status, results of hormonal receptor study were available in 69.5 % (248/357) of cases. Of these patients, ER and/or PgR were positive in 62.1% (154/248). ER and PgR were both negative in 37.9% (94/248). Adjuvant hormonal therapy was given to 34.2% (122/357) of all patients. There were 17.1% (61/357) of patients received both adjuvant chemotherapy and hormonal therapy. Patients who did not received any adjuvant treatment were 12.6% (45/357).

Table 1 Policy of adjuvant treatment scheme in early breast cancer patients who underwent mastectomy between 1991 and 2001 at Radiation Oncology Unit, King Chulalongkorn Memorial Hospital.

- **Adjuvant radiation therapy**
  1. chest wall alone in
     - close margin less than 2 mm
     - positive resected margin
     - large tumor (T3) without axillary node involvement
  2. chest wall + supraclavicular lymph node field in
     - high risk with axillary node positive less than 4 lymph nodes
- **Adjuvant chemotherapy in**
  - positive axillary lymph nodes
  - tumor size larger than 1 cm
  - high grade tumor
  - negative ER and PgR
- **Adjuvant hormonal therapy in**
  - positive ER and/or PgR

Table 2 Patient characteristics

	N	(%)
Age		
< 35	30	8.4
35-49	157	44.0
50-69	151	42.3
>70	19	5.3
Pathological T-stage		
T1	72	20.2
T2	239	66.9
T3	46	12.9
T4	-	-
Number of pathological positive lymph nodes		
Negative	156	43.7
N1-3	87	24.4
N4-9	74	20.7
N10 or more	33	9.2
positive node (unspecified number)	7	2
Stage grouping		
I	39	10.9
IIA	132	37.0
IIB	152	42.6
III	34	9.5
Grade		
Unknown	157	44.0
Known grade	200	56.0
G1	17	8.5
G2	113	56.5
G3	70	35.0
Estrogen receptor		
Unknown	118	33.1
Known	239	66.9
Negative	103	43.1
Positive	136	56.9

N = Number of patients

Progesterone receptor		
Unknown	142	39.8
Known		
Negative	113	52.6
Positive	102	47.4
Margin of resection		
> 2 mm	328	91.9
≤ 2 mm	16	4.5
Positive margin	11	3.1
Unknown	2	0.6

Table 3 Correlation between T stage and number of positive axillary lymph nodes

	N0 n (%)	N1-3 n (%)	N4-9 n (%)	N ³10 n (%)	positive node (unspecified) n (%)	Total n
T1	39 (54.2%)	20 (27.8%)	10 (13.9%)	2 (2.8%)	1 (1.3%)	72
T2	100 (41.8%)	62 (25.9%)	48 (20.1%)	23 (9.6%)	6 (2.6%)	239
T3	17 (36.9%)	5 (10.9%)	16 (34.8%)	8 (17.4%)	0 (0%)	46
Total	156	87	74	33	7	357

Note: N 0 : No axillary lymph node involvement
N1-3 : one to three positive nodes
N 4-9 : four to nine positive nodes
N ≥10 : ten or more than ten positive nodes
Positive node (unspecified) : Positive lymph node but unspecified number

Table 4 Adjuvant therapy given to the patients

Adjuvant Treatment	N	(%)
Adjuvant radiation		
No	160	44.8
Yes	197	55.2
Adjuvant chemotherapy		
No	110	30.8
Yes	247	69.2
CMF	151	61.1
Anthracycline-based	87	35.2
Other	9	3.6
Adjuvant Hormonal treatment		
No	235	65.8
Yes	122	34.2
- Tamoxifen	118	96.7
- Others	4	3.3
Both chemotherapy and Hormonal treatment	61	17.1
No any adjuvant treatment	45	12.6

Overall survival and relapse-free survival rates (Table 5 and 6)

The 5-year overall survival and relapse-free survival rates for the whole group were 72.3% and 58.6%, respectively (Figure 1 and Figure 2). For stage I, IIA, IIB and IIIA, the 5-year overall survival rates(Table 5) were 75.2%, 81.0%, 69.0% and 49.8%, respectively (P= 0.0001). The corresponding 5-year relapse-free survival rates were 53.9%, 68.1%, 57.5%, and 32.1%, respectively (P = 0.0017).

Comparison between negative- and positive-axillary lymph node

The median number of dissected axillary lymph nodes was 15 nodes. According to the number of positive nodes, there were 43.7%, 24.4%, 20.7% and 9.2% of the patients who had 0, 1-3, 4-9 and ≥10 positive nodes, respectively (Table 3). Seven patients (2%) did not have specified number of positive axillary node.

Five-year overall survival rates were 79.7%, 76.6%, 62.9% and 49.1% for patients with NO, N1-3, N4-9 and N≥10, respectively (P=0.0024) (Table 5). The corresponding relapse-free survival rates were 64.7%, 63.4%, 49.8% and 40.8%, respectively (P=0.0065) (Table 6).

Comparison of other disease status

Subgroup analyses of patients stratified by adjuvant radiation (no or yes), adjuvant chemotherapy

(no or yes) and chemotherapy regimens (CMF or anthracycline-based) were performed. The 5-year overall and relapse-free survival rates are demonstrated in table 5.

Factors significantly affect overall survival rate composed of stage, T-stage, number of positive lymph node and regimens of chemotherapy. While factors significantly affect relapse-free survival rate composed of stage, number of positive lymph node and adjuvant radiation therapy.

Patients who received adjuvant radiation therapy had statistically significant superior 5-year relapse-free survival rate as compared to those who did not received adjuvant radiation therapy (66.2 % vs 50.2 %). However, 5-year overall survival rates were comparable (72.1% vs 72.1%).

Five-year overall survival rates in patients who received and did not received adjuvant chemotherapy were 70.3% and 75.8% (P= 0.26), respectively. The corresponding 5-year relapse-free survival rates were 61.2% and 54.4% (p=0.21), respectively.

When stratified by the status of axillary lymph node involvement (Table 6), there was no statistically significant survival difference between the patients who received and those who did not received adjuvant chemotherapy. The survival rates in anthracycline-based chemotherapy subgroup were not superior to CMF regimen subgroup in term of 5-year overall survival or relapse free survival rates.

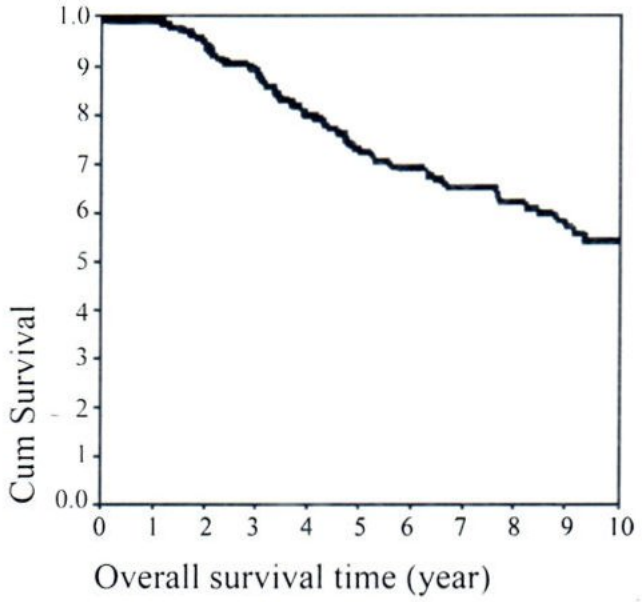

Figure 1 Overall survival curve

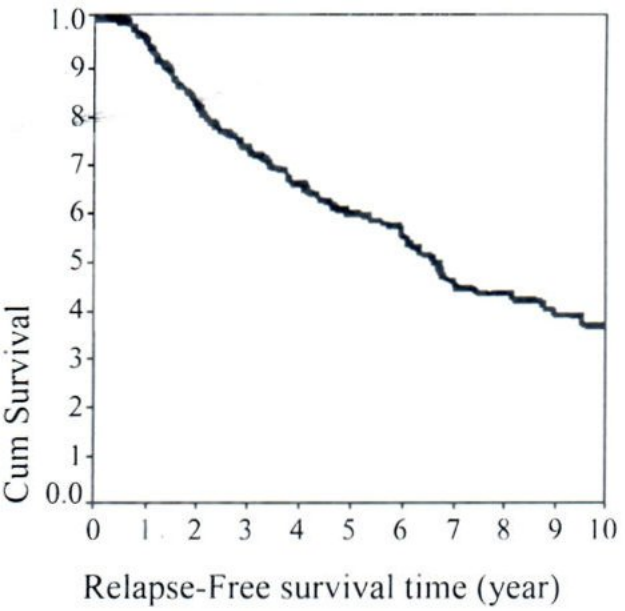

Figure 2 Relapse-free survival curve

Table 5 Five-year overall survival and relapse free survival rates stratified by groups

Group	Number	5-yearP-value Overall survival % (SE*)	P-value	5-year relapse -free survival % (SE*)	P-value
Stage					
I	39	75.2 (8.9)	0.0001	53.9 (10.2)	0.0017
IIA	132	81.0 (4.3)		68.1 (4.8)	
IIB	152	69.0 (4.8)		57.5 (5.0)	
IIIA	34	49.8 (10.4)		32.1 (9.3)	
T-stage					
T1	72	77.8 (6.4)	0.0187	59.8 (7.3)	0.141
T2	239	73.1 (3.6)		61.4 (3.7)	
T3	46	60.2 (9.3)		40.7 (9.4)	
Nodal status					
Negative	156	79.7 (4.1)	0.0024	64.7 (4.7)	0.0065
Positive	201	66.4 (4.2)		54.0 (4.3)	
1-3	87	79.7 (4.1)		63.4 (6.5)	
4-9	74	62.9 (7.4)		49.8 (7.0)	
≥10	33	49.1 (11.2)		40.8 (7.0)	
⊕ unspecified**	7	57.1 (18.7)		42.9 (18.7)	
Adjuvant radiation					
Yes	197	72.1 (4.1)	0.97	66.2 (4.1)	0.0003
No	160	72.1 (4.4)		50.2 (4.8)	
Adjuvant chemotherapy					
Yes	247	70.3 (3.9)	0.263	61.2 (3.8)	0.21
No	110	75.8 (4.7)		54.4 (5.5)	
Chemotherapy regimens					
CMF	151	75.9 (4.5)	0.0059	65.7 (4.7)	0.0548
Anthracycline	87	62.7 (7.7)		57.2 (6.8)	
Other	9	35.0 (19.7)		18.8 (16.7)	

* SE – Standard error

** Positive lymph node but unspecified number

Table 6 Five-year overall and relapse-free survival rates stratified by nodal status and chemotherapy regimens

	N	5-yr Overall survival rate %(SE)*	P-value	5-yr relapse-free survival rate % (SE)*	P-value
LN negative					
Adj Chemo					
Yes	84	80.0 (5.2)	0.799	70.2 (6.5)	0.1592
No	72	78.3 (6.7)		60.4 (6.5)	
LN negative**					
CMF	74	78.0 (7.2)	0.6892	69.7 (7.0)	0.8021
Anthra***	9	75.0 (21.7)		74.1 (16.1)	
LN positive					
Adj Chemo					
Yes	163	66.6 (4.8)	0.924	57.15 (4.6)	0.1977
No	38	65.7 (9.7)		41.0 (10.1)	
LN. positive**					
CMF	77	73.9 (5.9)	0.116	62.4 (6.3)	0.3118
Anthra***	78	60.4 (8.4)		55.1 (7.4)	

* SE - Standard error

** Patients received chemotherapy other than CMF and anthracycline-based regimens were not included

*** anthracycline-based regimen

DISCUSSION

This retrospective study revealed 5-year overall and relapse-free survival rates of 72.3% and 58.6%, respectively. As we know that the most established prognostic factors are the involvement and the number of positive axillary lymph nodes based on adequate dissection of level I and II axillary nodes. When the number of involved nodes increase; relapse rates increase and survival rates decrease.[12] The current study showed statistically significant decrease in overall and relapse-free survival when the number of positive axillary lymph nodes increased.

When T-stage and axillary lymph node were grouped by AJCC 1997 stage grouping,[11] we found statistically significant difference in survival rates among different stages. The 5-year overall survival rates reported in the National Cancer Data Base for the year 1989[11] were 87%, 78%, 68% and 51% for stage I, IIA, IIB and IIIA, respectively. While the corresponding rates in our study were 75.2%, 81.0%, 69.0% and 49.8%, respectively.

The Early Breast Cancer Trialists[13] evaluated

the effect of adjuvant polychemotherapy in 2,710 node-negative breast cancer patients. The 5-year disease-free survival rates were 67% and 75% for control and adjuvant chemotherapy groups, respectively. Our current study showed that 5-year relapse-free survival rate in node-negative patients who did not receive chemotherapy was 60.4%, while it was 70.2% in the adjuvant chemotherapy group (table 6).

In the updated report of the Early Breast Cancer Trialists[6] regarding patients with negative lymph node and under 50 years of age, the five-year survival rates were 83.5% and 86.5% for control and adjuvant chemotherapy groups, respectively. The corresponding survival rates in the 50-69 year-old group were 81.4% and 85.3%. Our result showed that 5-year overall survival rates in node-negative patients were 78.3 % and 80% for those who did not receive and those who received adjuvant chemotherapy, respectively. Although patients who received chemotherapy had worse prognostic factor, the 5-years overall survival rates were not inferior. This result underlined the benefit of adjuvant chemotherapy.

For patients with negative axillary lymph node, Fisher et al (NSABP B-23 trial)[14] reported 5-year overall survival rates of 89% for patients treated with CMF and 90% for those treated with AC (doxorubicin plus cyclophosphamide) (P = 0.04). The 5-year relapse-free survival rates were identical, 87%, for both CMF and AC treated groups. Regardless of chemotherapy regimens, the patients with negative axillary lymph node in our study had a better comparable 5-year overall survival and relapse-free survival. However, this result should be interpreted with caution because of the small number of patients in anthracycline-based subgroup.

Bang[15] reported the study in positive axillary lymph node patients. The patients were randomized between adjuvant AC (doxorubicin plus cyclophosphamide) and CMF. The 5-year overall survival rates for AC group and CMF group were 90% and 86%, respectively(P=0.96). The corresponding 5-year recurrence-free survival rates were 64% and 78% (P=0.12).

Levine[16] randomized premenopausal women with node-positive breast cancer between adjuvant intensive CEF (cyclophosphamide, epirubicin and 5-FU) and CMF (classical). The five-year survival rates for CEF and CMF groups were 77% and 70%, respectively(P=.03). Whereas 5-year relapse-free survival rates were 63% and 53%(P=.009).

French Adjuvant Study Groups[17]reported 565 operable breast cancer patients with positive lymph nodes between adjuvant FEC50 and FEC100 for 6 cycles. The 5-year overall survival rates were 65.3% for FEC50 and 77.4% for FEC100 (P = 0.03). The 5-year disease-free survival rates were 54.8% and 66.3%, respectively(P=.03).

The recent report by Henderson[18] showed that the 5-year overall survival rates were 77% after adjuvant AC (doxorubicin plus cyclophosphamide) and 80% after AC plus paclitaxel. The corresponding disease-free survival rates were 65% and 70%, respectively.

In the Early Breast Cancer Trialists' overview of polychemotherapy, comparison of anthracycline-containing regimens with CMF showed a 12% further reduction in the annual odds of recurrence(= 0.006) and an 11% further reduction in the annual odds of death (= 0.02) with anthracycline-containing regimens.[6] Based on the above study, the NCCN guideline suggested that anthracycline-containing regimens are preferred for node positive patients.[19]

Our results in patients with positive axillary lymph node showed that 5-year overall survival rate was 65.7% in patients who did not receive adjuvant chemotherapy, while they were 73.9% and 60.4% in patients who received adjuvant CMF and anthracycline-based regimens, respectively. The 5-year relapse-free survival rates were 41.0%, 62.4% and

55.1%, respectively. Since the patients who received anthracycline-based chemotherapy regimen had worse prognostic factors than those who received CMF regimen in our study, this explained the inferior overall survival of anthracycline-based regimen.

CONCLUSION

Overall, our results of breast cancer treatment at Radiation Oncolgy Unit, King Chulalongkorn Memorial Hospital were comparable to the previous reports in medical literatures. The improvement on diagnostic, pathological and treatment procedures will enhance survival rates in the near future. This study provided a base line data of breast cancer treatment results in Thailand, King Chulalongkorn Hospital.

REFERENCES

1. S. Deerasamue, N. Martin, S. Sontipong, et al. Cancer in Thailand Vol II, 1992-1994.(IARC Scientific Publications No.145), Lyon, IARC.
2. Srilung H, Sontipong S, Martin N, et al. Cancer in Thailand 1995-1997 Vol. III: 47-48
3. Tumor Registry Statistical Report 2000. King Chulalongkorn Memorial Hospital.
4. Tumor Registry Statistical Report 2001. King Chulalongkorn Memorial Hospital.
5. Cancer in Siriraj 1990-1999. Cancer Registry. Faculty of Medicine Siriraj Hospital. Mahidol University.
6. Early Breast Cancer Trialists' Collaborative Group. Polychemotherapy for early breast cancer: an overview of the randomised trials. Lancet 1998; 352: 930-42.
7. Early Breast Cancer Trialists' Collaborative Group. Tamoxifen for early breast cancer: an overview of the randomised trials. Lancet 1998; 351:1451-67.
8. Lertsanguansinchai P, Lertbutsayanukul C, Chatamra K, et al. Pattern of local-regional recurrence in patient with early breast cancer after mastectomy: an analysis of 357 cases at King Chulalongkorn Memorial Hospital. J Med Assoc Thai 2004; 87: S168-S174
9. Kaplan EL, Meier P. Nonparametric estimation from incomplete observations. J Am Stat Assoc 1958; 53: 457-481.
10. Mantel N. Evaluation of survival data and two new rank order statistics arising in its consideration. Cancer Chemother Rep 1966; 50: 163-170.
11. American Joint Committee on Cancer. AJCC Cancer staging manual. Philadelphia: Lippincott-Raven, 1997: 171-178.
12. Saez RA, McGuire WL, Clark GM. Prognostic factors in breast cancer. Semin Surg Oncol 1989; 5: 102-110
13. Early Breast Cancer Trialists' Collaborative Group. Systemic treatment of early breast cancer by hormonal, cytotoxic or immune therapy. 133 randomized trials involving 31,000 recurrences and 24,000 deaths among 75,000 women. Lancet 1992; 339: 71-85.
14. Fischer B, Anderson S, Tan-Chiu E, et al. Tamoxifen and chemotherapy for axillary node-negative, estrogen receptor-negative breast cancer: findings from National Surgical Adjuvant Breast and Bowel Project B-23. J Clin Oncol 2001; 19: 931-942.
15. Bang SM, Heo DS, Lee KH, et al. Adjuvant doxorubicin and cyclophosphamide versus cyclophosphamide, methotrexate, and 5 -fluorouracil chemotherapy in premenopausal women with axillary lymph node positive breast carcinoma. Results of a randomized controlled trial. Cancer 2000; 89: 2521-2526.

16. Levine MN, Bramwell VH, Pritchard KI, et al. Randomized trial of intensive cyclophosphamide, epirubicin, and fluorouracil chemotherapy compared with cyclophosphamide, methotrexate, and fluorouracil in premenpausal women with node-positive breast cancer. National Cancer Institute of Canada Clinical Trials Group. J Clin Oncol 1998; 16: 2651-2658.

17. The French Adjuvant Study Group. Benefit of a high-dose epirubicin regimen in adjuvant chemotherapy for node-positive breast cancer patients with poor prognostic factors: 5-year follow-up results of French Adjuvant Study Group 05 randomized trial. J Clin Oncol 2001; 19: 602-611.

18. Henderson IC, Berry DA, Demetri GD, et al. Improved outcomes from adding sequential paclitaxel but not from escalating doxorubicin dose in an adjuvant chemotherapy regimen for patients with node-positive primary breast cancer. J Clin Oncol 2003; 21: 976-983.

PATIENT SKIN DOSE MEASUREMENT IN CARDIAC CATHETERIZATION AND INTERVENTIONAL RADIOLOGY

KRISANACHINDA A,[1] KUMKRUA C,[1] WANGSUPHACHART S[1]

ABSTRACT

Objective: To determine the skin dose received by the patients who underwent cardiac catheterization and interventional radiology.

Methods: The patient skin dose in this study was determined by radiochromic film and Dose Area Product (DAP) methods. The dose measurement was carried out in 64 adult patients who underwent the interventional radiology examinations such as transarterial oily chemo embolization (TOCE), percutaneous transhepatic biliary drainage (PTBD), neurovascular intervention/angiography and percutaneous transluminal coronary angioplasty/stent (PTCA) at King Chulalongkorn Memorial Hospital. The maximum entrance skin dose from each case was determined by scanning radiochromic film to get the maximum density area on the film. This area represented the maximum entrance dose. However, the comparison of the radiochromic film and DAP were made to assess the patient skin dose and the maximum radiation dose from each procedure.

Results: The maximum skin dose from transarterial oily chemo embolization (TOCE) was 365 cGy, percutaneous transhepatic biliary drainage (PTBD) was 183 cGy, percutaneous transluminal coronary angioplasty/stent (PTCA) was 294 cGy, neurovascular interventional was 180 cGy and neurovascular angiography was 110 cGy. The patient skin dose in these studies depend on the length of fluoroscopy time and only one patient who reached the threshold dose of skin injury of 300 cGy. The maximum skin dose assessment from radiochromic film was compared with DAP calculation and showed the agreement, but radiochromic film showed higher radiation dose, because the calculated dose from DAP was the accumulated skin dose at different area and it was not the point entrance area of the patient.

Conclusions: There was only 1 incident where maximum skin dose exceeded the threshold dose for temporary epilation. The determination of the radiation dose in interventional radiology and cardiac catheterization is a benefit for the prevention of radiation skin injury and also increase the awareness of the radiologist and cardiologist in using the radiation for interventional procedures.

[1] Department of Radiology, Faculty of Medicine, Chulalongkorn University, Bangkok Thailand

INTRODUCTION

An increasing number of invasive procedures, primarily therapeutic in nature and involving uses of devices under fluoroscopic guidance, are becoming accepted in medical practice. Examples of such procedures are Percutaneous Transluminal Coronary Angioplasty/Stent (PTCA), neurointerventional radiology and catheter-based hepatobiliary interventional procedures including transarterial oily chemoembolization (TOCE) and percutaneous transhepatic biliary drainage (PTBD). These procedures are performed by a variety of medical specialists and may provide significant advantages over alternative therapies in terms of improved clinical outcome and reduced overall patient risks. However, physicians performed these procedures should be aware of the potential for serious radiation-induced skin injury caused by long periods of fluoroscopy occurring with some of these procedures. Such injuries have recently been reported as a result of radiation exposure during some of these procedures due to long fluoroscopic exposure times, high dose rates or both.

The radiochromic film known as Gafchromic film in this study was long widely used as a patient radiation dose detector.[1] It was applied to determine the doses in radiation therapy for many regions of the body i.e. breast.[2] The Gafchromic film was used in some study to measure the dose distribution in water in comparison to a solid phantom.[3] Some study showed the sensitivity of the Gafchromic film[4] and the application in radiation therapy. The Gafchromic film used in this study is the new type that develop for low dose detection for diagnostic purposes.

The other method for patient dose assessment is the use of Dose Area Product (DAP) meter, which the detector will be placed on the housing of the x-ray tube. The read out data from DAP meter in $cGy.cm^2$ and the radiation area in cm^2 from the verification film is calculated to determine the patient skin dose (cGy). The clinical research conducted at the cardiac center and the section of vascular & interventional radiology at King Chulalongkorn Memorial Hospital where the clinical service on cardiac catheterization such as PTCA, neurointerventional radiology and catheter-based hepatobiliary interventional procedures including TOCE and PTBD have been routinely performed and employs fluoroscopy.

In this study the Gafchromic film was used to determine the maximum entrance dose, DAP method was used to determine the total radiation dose of each procedure. Using both data from Gafchromic film and DAP method to determine and calculate the patient skin dose.[5]

EQUIPMENT AND ACCESSORIES

1 Gafchromic XR Type R Film (Model 37-046)

Gafchromic XR Type R is a self-developing radiochromic film. The film has white opaque at one side and yellow on the other side. The color of the yellow side will be changed to green color and darker as proportional to the amount of radiation doses in the range of 0.2 - 15 Gy.[6] The film is not energy dependent between 60 keV-120 keV, outstanding uniformity, dose rate and fractionation independent. This film type is designed and can be used to improve fluoroscopic technique and patient safety.[5,7]

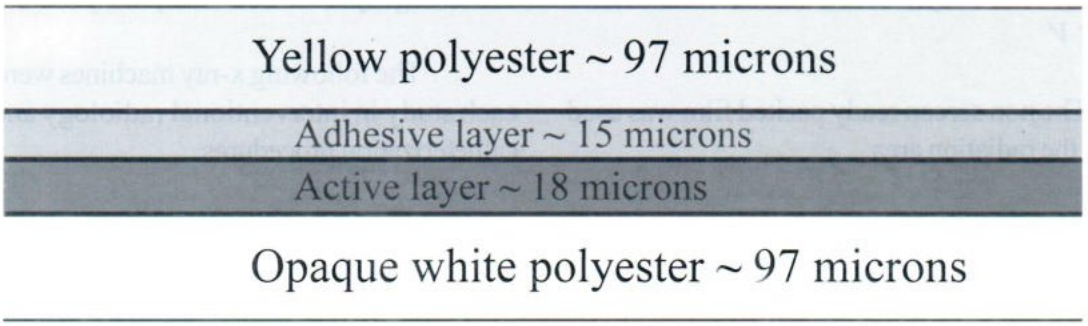

Fig.1 Configuration of Gafchromic XR Type R film

2 Dose Area Product (DAP) Meter (MODEL PTW-Diamentor E)

Dose-Area-Product (DAP) meter is large -area, transmission ionization chamber and associated electronics. In use, the ionization chamber is placed perpendicular to the beam central axis and in a location to completely intercept the entire area of the x-ray beam and the meter is placed at the control area. The DAP, in combination with information on x-ray field size (FOV) can be used to determine the average dose produced by the x-ray beam at any distance downstream in the x-ray beam from the location of the ionization chamber.

DAP meter is used to measure the absorbed dose (cGy), times the area of the x-ray field (cm^2), on patient skin. The relationship between DAP and exposure-area product (EAP) is essentially a single conversion factor that relates dose to exposure. EAP is expressed in roentgen-cm^2 (R-cm^2) and DAP is expressed in gray-cm^2 (Gy-cm^2,usually read in cGy -cm^2). The reading from a DAP meter is affected by the exposure factors (kVp, mA, or time), the area of the field (FOV), or both. The chamber area must be larger than that of the collimators, as the collimation blades are opened or closed, the charge collected will also increase or decrease in proportion to the area of the field.

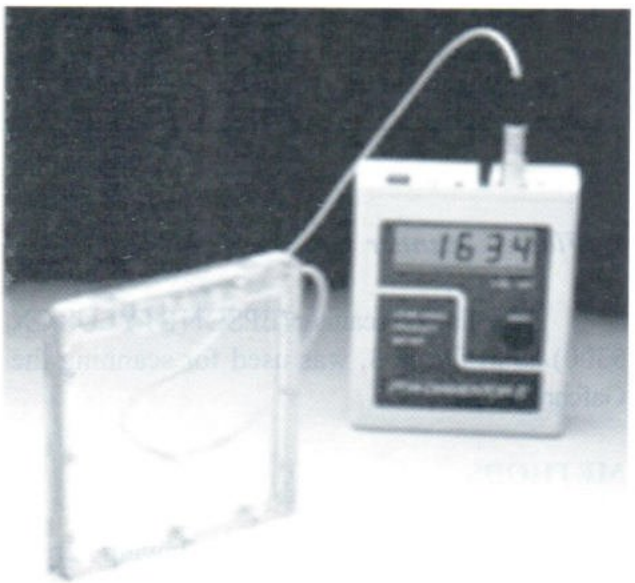

Fig.2 DAP meter and the Ion Chamber

3.Portal Film (Verification Film) Kodak Model X-Omat V

The non screen ready packed film was used to verify the radiation area.

4. Radiographic/Fluoroscopic System

The following x-ray machines were used for each study in interventional radiology and cardiac catheterization procedures.

Table 1 The equipment used for each procedure.

Procedures	Manufacturer	Model
1. Abdominal Interventional Radiology		
1.1. Transarterial Oily Chemoembolization (TOCE)	Siemens	Polystar
1.2. Percutaneous Transhepatic Biliary Drainage (PTBD)		
2. Neurovascular Interventional Radiology	Siemens	Neurostar
3. Percutaneous Transluminal Coronary	Siemens	Coroskop
Angioplasty / Stent (PTCA)	Siemens	Axiom

5. Flatbed Scanner

The flatbed scanner (EPSON STYLUS CX 5300) as in figure 3, was used for scanning the Gafchromic film.[5,7]

METHODS

The study was carried on as these following steps.

1. The evaluation of radiographic-fluoroscopic system performance.[8,9]
2. The calibration of Gafchromic film and DAP meter.
3. The patient data collection using Gafchromic film and DAP meter methods.
4. The analysis of the data.
5. The evaluation of the patient skin dose.

Fig.3 Flatbed scanner

RESULT

Table 2 The results of the clinical study showing the maximum skin dose measured by Gafchromic film and the skin area dose measured by DAP meter

Studies	x-ray tube	No.of cases	Age (Years)	Skin Dose from GF (cGy)	Radiation Area (cm2)		Flu Time (min)		DAP (cGy.cm2)	
				Max	Max	Min	Max	Min	Max	Min
TOCE		21	36-72	365	431	52	48	2.4	38,168	2,433
PTBD		5	17-87	183	186	82	15.03	1.51	5,972	520
Neuro	A			165	260	153	46	3.7	26,378	2,689
	B			165	285	153	21		16,825	1,176
	Total	22	17-61	180	285	153	46	3.7	36,221	3,865
PTCA		16	42-79	294	135	36	17.2	0.8	20,000	3,050
Total		64								

Fig 4: Maximum Skin Dose of Each Procedure

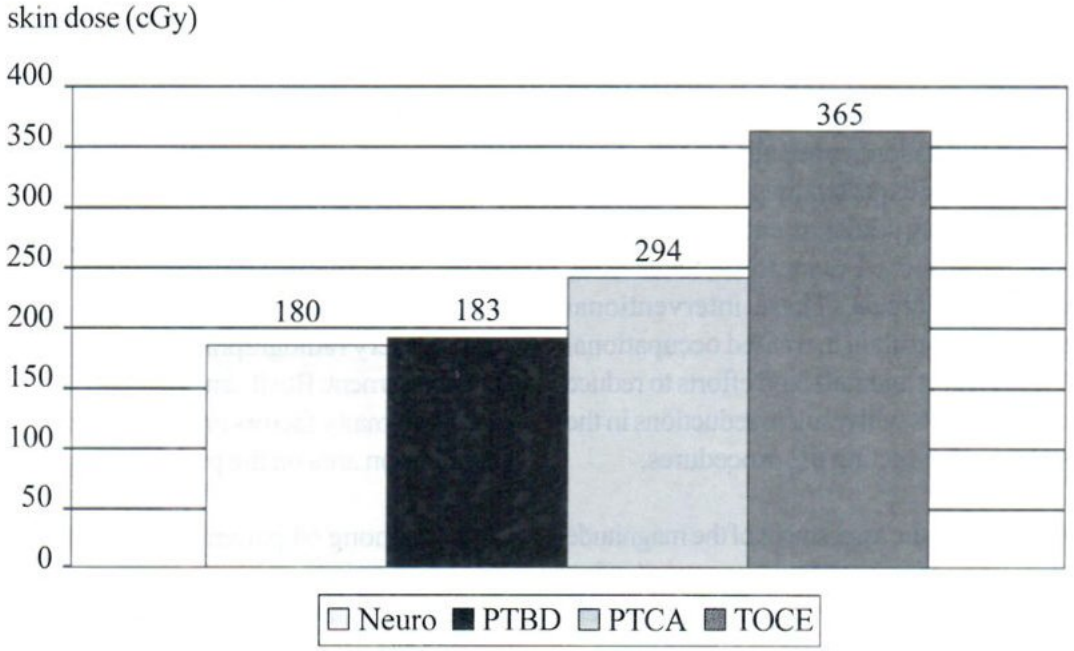

Fig.4 shows the results of the study as the data in the table 2 performed on 64 patients, the maximum skin dose was recorded from the TOCE procedure as 365 cGy, PTCA procedure 294 cGy. The longest of fluoroscopic time, 48 minutes was recorded from the TOCE procedure.

DISCUSSION

The result shows the linear correlation between the estimated dose from DAP meter and the maximum skin dose from Gafchromic film. There are several factors affected the dose estimation by the DAP meter such as the variation of the radiation field, the angle of the x-ray tube, varying the x-ray shutter during fluoroscopy, those made uncertain area for dose estimation.

The maximum skin dose determined by Gafchromic film of each procedure is higher than the estimated dose from DAP meter. Because the DAP is the cumulative dose from every exposure to parts of the patient, so the dose could be estimated from the averaged radiation areas, while maximum dose measured at one point on exposed skin. Both results compliment to each other and benefit the patient except the maximum exceeds the threshold level of skin injury.

Interventional radiology and cardiac catheterization procedures may increase the risk for late effects such as radiation-induced skin injuries. The potential for such late effects should not be disregarded in risk/benefit considerations, especially for individuals with many decades of expected life remaining, such as pediatric and young adult patients, or for procedures involving absorbed dose to radiosensitive tissues such as the breast. These interventional procedures can also result in increased occupational exposure to physicians and staff, and efforts to reduce the exposure to patients will result in reductions in the exposure to those conducting the procedures.

Complicating the assessment of the magnitude of the problem of injuries from fluoroscopy is the fact that the injuries are not immediately apparent. Typical times to onset or appearance of the effect may appear at variable period. The mildest symptoms, such as transient erythema, the effects of the radiation may not appear until weeks following the exposure. Physician performing these procedures may not be in direct contact with the patients following the procedure and may not observe the symptoms when they occur. Missing the milder symptoms in some patients can lead to surprise at the magnitude of the absorbed doses delivered to the skin of other patients when more serious symptoms appear. For this reason, it is recommended that information be recorded in the patient's record which permits estimation of the absorbed dose to the skin. Conside- ration should be given to counseling such patients on the possible symptoms and risks from those procedures.

CONCLUSION

The Gafchromic film detector has adequately measured maximum skin dose during fluoroscopic procedure for the interventional radiology and cardiac catheterization.[5,7] It can provide information for point dose assessment or profile measurements of dose if required but the relative expense of the film is a main obstacle.

The DAP meter is convenience instrument for radiation dose estimation and it generally should be built in every radiographic-fluoroscopic system for dose assessment. But it can be over or under estimated caused by many factors and the difficulty in located the radiation area on the patient.

Among 64 patients, there is 1 of the patient who has maximum skin dose exceed the threshold dose for temporary epilation[5] as shown in Table 3

Table 3 Radiation induced skin injuries

Effect	Typical Threshold Absorbed Dose (Gy)*	Hours of Fluoroscopic "On Time" to reach threshold+ at:		Time to Onset of Effect++
		Usual Fluoro. Dose Rate of 0.02 Gy/min (2 rad/min)	High-Level Dose Rate of 0.2 Gy/min (20 rad/min)	
Early transient erythema	2	1.7	0.17	Hours
Temporary epilation	3	2.5	0.25	3 wk
Main erythema	6	5.0	0.50	10 d
Permanent epilation	7	5.8	0.58	3 wk
Dry desquamation	10	8.3	0.83	4 wk
Invasive fibrosis	10	8.3	0.83	
Dermal atrophy	11	9.2	0.92	>14 wk
Telangiectasis	12	10.0	1.00	>52 wk
Moist desquamation	15	12.5	1.25	4 wk
Late erythema	15	12.5	1.25	6-10 wk
Dermal necrosis	18	15.0	1.50	>10 wk
Secondary ulceration	20	16.7	1.67	>6 wk

* The unit for absorbed dose is the gray (Gy) in the International System of units. One Gy is equivalent to 100 rad in the traditional system of radiation units.

\+ Time required to deliver the typical threshold dose at the specified dose rate.

++ Time after single irradiation to observation of effect.

The determination of the radiation dose in the interventional radiology and cardiac catheterization is valuable for radiation injury prevention and also increase the awareness of the radiologist and cardiologist.

The result can be used as a guideline for studying the dose range of each procedure (Table 2) in order to optimize the exposure technique and the dose limit.

REFERENCES

1. Butson M J, Mathur J N, and Metcalfe P E. Radiochromic film as a radiotherapy surface dose detector. Phys Med Biol 46,1996; 235-240.
2. Cheung T, Butson M J, and Yu P K N. Multilayer Gafchromic film detectors for breast skin dose determination in vivo. Phys Med Biol 47, 2002; 31-37.
3. Butson M J, Cheung T, and Yu P K N. Radiochromic film dosimetry in water phantoms. Phys Med Biol 46, 2001; 27-31.
4. Butson M J, Cheung T, and Yu P K N. Corresponding dose response of radiographic film with layered Gafchromic film. Phys Med Biol 47, 2002; 285-289.
5. Food and Drug Administration, "Important Information for Physicians and Other Health Care Professionals" Recording Information in the Patient's Medical Record that Identifies the Potential for Serious X-Ray Induced Skin Injuries Following Fluoroscopically Guided Procedures, September15th, 1995.
6. Fajardo LC, Geise RA, Ritenour ER. A survey of films for use as dosimeters in interventional radiology. Health Phys 68, 1995; 595-599.
7. Thomas G, Chu RY, and Rabe F. A study of Gafchromic XR Type R film response with reflective-type densitometers and economical flatbed scanners. Appl Clin Med Phys.4, 2003; 307-314.
8. American Association of Physicists in Medicine, Managing the use of fluoroscopy in medical institutions, AAPM Report No. 58, 1998; 1 37.
9. Shope TB. "Regulations and recommendations relevant to interventional radiology" in Syllabus: categorical course in physics: physical and technical aspects of angiography and interventional radiology (Oak Brook, Radiological Society of North America, 1995; 195-205.

PROSTATIC ABSCESS

DR. M.A. TAHER[1]

INTRODUCTION

Prostatic abscesses develop secondary to prostatitis or surgical manipulation, e.g. transurethral resection of the prostate or cystoscopy. Prostatitis is an inflammatory condition of the prostate that can affect men of all ages following puberty. Most cases of primary prostatitis involve the peripheral prostate, except following surgical manipulation. Thus, abscesses can develop peripherally or centrally. Abscesses will generally be anechoic or hypoechoic with relatively sharp margins and good sound transmission, suggesting the predominantly fluid nature of the collection. Because much of the fluid may be complicated (i.e. purulent material), echoes within the mass may be seen and the walls may be thick.[1]

CASE REPORT

A young man of 35 years came with fever and abdominal pain. Ultrasound scan (3.7 MHz) showed a 23.1 mm echo-free area in the prostate gland (Fig.1). The patient was diagnosed as a case of prostatic abscess, and was improved after 500 mg single daily dose of levofloxacin for three days.

DISCUSSION

Prostatitis is a clinical diagnosis; imaging is irrelevant.[2] In prostatic abscess a transrectal sonogram, needle aspiration and drainage may be needed, however, in the case presented here, transabdominal ultrasound was enough to make a correct diagnosis and the patient was cured by conservative management

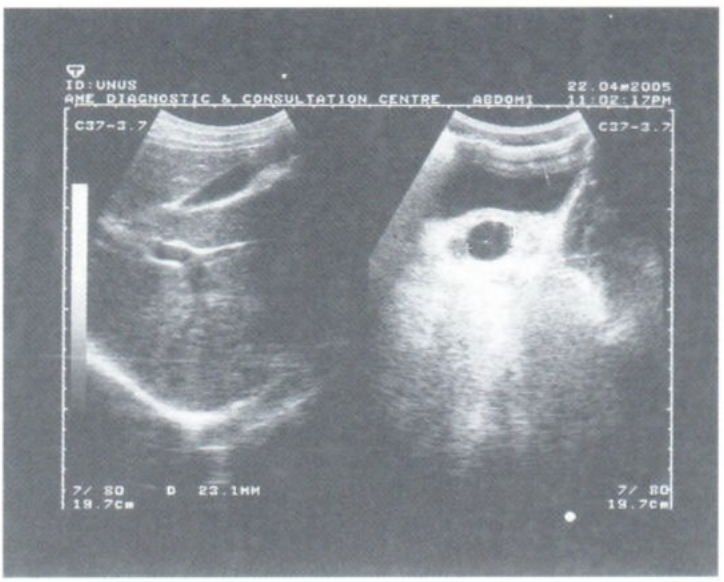

Fig.1 Prostatic abscess.

[1] Director & Chief Madical Officer, Centre for Nuclear Medicine & Ultrasound, Rangpur-5400, Bangladesh.

REFERENCES

1. Rifkin MD, Prostate. In Goldberg BB (ed.): Textbook of Abdominal Ultrasound. Williams and Wilkins. Baltimore 1993, pp. 418-451.

2. Thomson HS, Pollack HM. The genitourinary system. In Pettersson H (ed.): The NICER Centennial Book 1995 A Global Text Book of Radiology, Oslo, pp. 1111-1216.

ISOTOPE RENOGRAM IN ECTOPIC KIDNEY

Dr. M. A. Taher[1]

ABSTRACT

Ultrasonography (USG), may provide some clue to diagnose an ectopic kidney, however, functional confirmation is best done by isotope renogram, as depicted by the rare cases reported below.

CASE REPORTS

Case 1

A young man of age 17 years complained of pain in left loin. Ultrasonography (USG) done elsewhere reported 'normal kidneys', but intravenous urography (IVU) revealed ectopic (pelvic) left kidney with mild hydronephrosis. Isotope renogram with technetium 99m DTPA (diethylenetriamine pentaacetic acid) showed normal right kidney and small ectopic left kidney just at the pelvic brim on the right side with mild obstruction. (Fig.1)

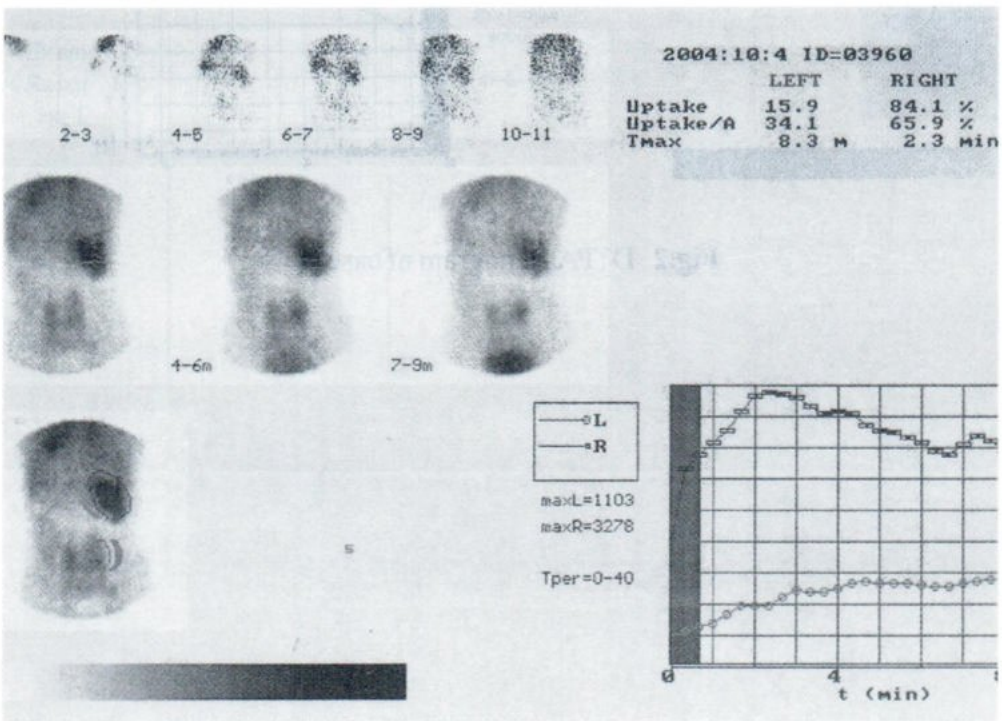

Fig.1 DTPA Renogram of case 1.

[1] Director, Centre for Nuclear Medicine and Ultrasound, Rangpur-5400, Bangladesh.

Case 2

A boy of 13 years presented with a painful mass in left loin. Left nephrostomy was done in January 2004 as it was the only kidney - - the patient did not have his right kidney since birth, but a large cystic mass was found in the mild-abdomen which was drained by Foley's catheter. DTPA renogram (Fig.2) on 26 Feb.2004 showed crossed ectopia with obstruction upto 40 minutes post-injection under computerized gamma camera (Siemens Germany). Follow up USG on 23 Nov 2004 showed moderate degree of pelvicaliectasis and the urologist surgeon planned to re-explore (Fig. 3)

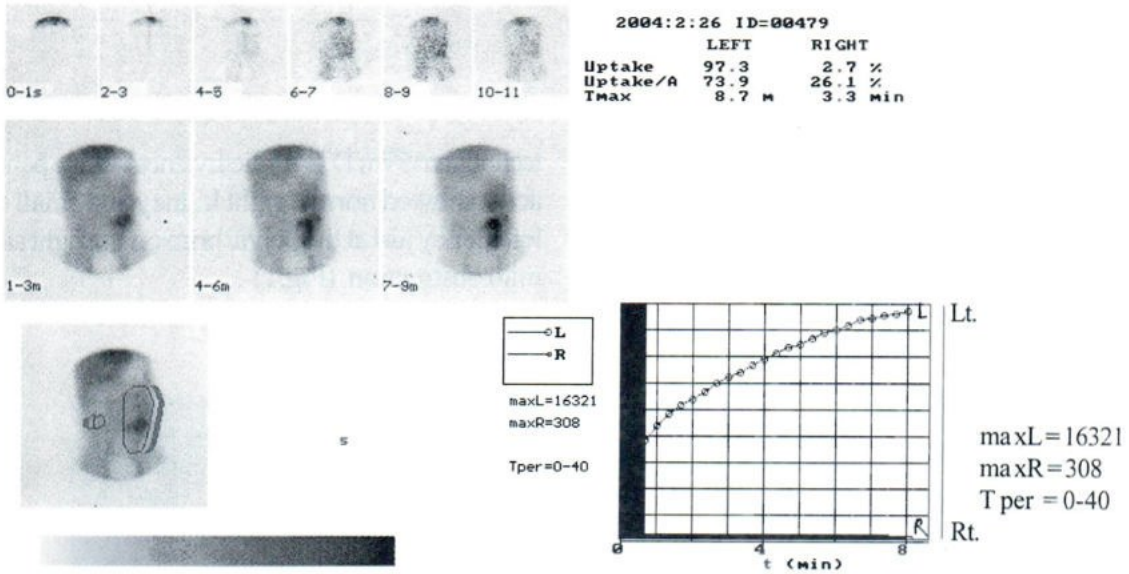

Fig.2 DTPA Renogram of case 2.

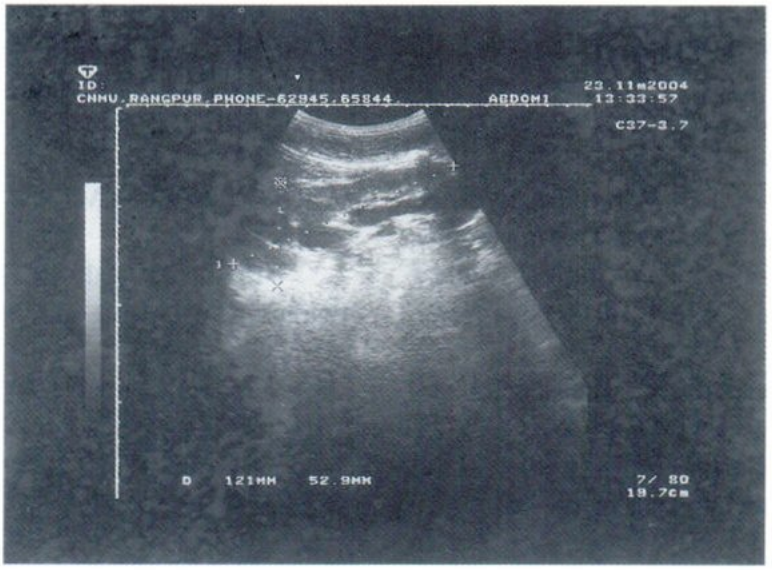

Fig.3 USG of LT. kidney.

INTRODUCTION

Ectopic kidney may be due to failure of complete ascent of the kidney from its primitive location at the 1st or 2nd sacral body level or excessive cranial migration beyond its normal location. Crossed renal ectopia is a condition in which the affected kidney is located entirely or primarily on the opposite side of the abdomen.[1] The ectopic kidney lies below the normal contralateral kidney, and the two organs are almost always fused. Approximately 50 cases of intrathoracic kidney have been reported-usually a mass is seen on chest x-ray and USG or CT demonstrates it to be a kidney.[2] A colon flexure or loop of small bowel may occupy the empty renal fossa mimicking a mass or kidney (pseudokidney sign).[3] Except for being displaced, most pelvic kidneys are normal. Occasionally, however a pelvic kidney is grossly abnormal in appearance because it is affected by dysplasia, duplication anomalies, vesicoureteral reflux and/or hydronephrosis. Diagnostic error may be avoided if the ipsilateral renal fossa is examined routinely in patients with pelvic pathology.[4] Radionuclide renal scan is valuable for the proper assessment of many congenital anomalies affecting the renal tract. The assessment of horse-shoe kidney or ectopic kidney can be done much more easily than with intravenous urography (IVU), because once the radioisotope has been given a whole-body search can be undertaken if necessary, whereas a small pelvic kidney, especially if it is poorly functioning, cannot always be seen against the background of the pelvic bone.[5] The spinal column may significantly attenuate low-energy gamma rays, so that anterior view of the kidneys may be wise.[6] Crossed fused ectopy may mimic a single kidney with a duplicated collecting system or a kidney with a renal mass.[7]

REFERENCES

1. Kirks DR, Laurin S. Pediatric radiology. In Pettersson H (ed.) A Global Text Book of Radiology. The NICER Institute, Oslo 1995 pp. 533-609.
2. Sumner TE, Volberg FM, Smolen PM Intrathoracic kidney-diagnosis by ultrasound. Pediatr Radiol 1982;12: 78-80.
3. McCarthy S, Rosenfield AT. Ultrasonography in crossed renal ectopia. J Ultrasound. Med 1984; 3 : 107-112.

4. Zwiebel WJ. Normal Variants and developmental anomalies of the urinary tract. In: Zwiebel WJ, Sohaey R. Introduction to Ultrasound, W. B. Saunders Co. Philadelphia 1998 pp. 176-185.
5. Britton KE, Maisey MN, Hilson AJW. Renal radionuclide studies. In Maisey MN, Britton KE, Gilday DL: Clinical Nuclear Medicine, Chapman and Hall, London,. 1983, pp. 93-133.
6. Tauxe WN. Dubovsky EV. The genitourinary system. In Harbert J, da Rocha AFG. Textbook of Nuclear Medicine vol. II Lea & Febiger, Philadelphia, 1994, pp. 481-521.
7. Neiman HL. The urinary system. In Goldberg BB (ed.): Textbook of Abdominal Ultrasound. pp. 330-388. Williams and Wilkins, Baltimore, 1993.

ACKNOWLEDGEMENT

Prof. Dr. Baharul Elem MBBS, FCPS (England) for valuable opinions and cooperations.

FOLLOW UP IMAGING AFTER PYELOPLASTY FOR URETEROPELVIC JUNCTION OBSTRUCTION (UPJO)

DR. M.A. TAHER[1]

ABSTRACT

Ultrasonography (USG) and radionuclide renography using technetium diethylene triamine pentaacetic acid (99m Tc DTPA) were done after pyeloplasty for ureteropelvic junction obstruction to confirm the individual renal functions in a young man of age 20 years, and a girl of 22 months.

INTRODUCTION

Approximately 1 in 100 pregnancies are noted to have fetal upper renal tract dilation on ultrasound. However, only 1 in 500 will be found to have significant urologic problems. UPJ obstruction is found in approximately 50% of patients diagnosed with antenatal hydronephrosis. Prior to the use of prenatal ultrasound, most patients with UPJ obstruction presented with pain, hematuria, urosepsis, failure to thrive, or a palpable mass. With the enhanced ability and availability of prenatal ultrasound, urologic abnormalities are being diagnosed earlier and more frequently. In 11-39% of patients, accessory renal vessels (artery alone or artery and vein) cross the UPJ, but this ureterovascular tangle is always associated with a fibrous intrinsic obstruction and may aggravate rather than initiate obstruction.[1,2] In some of these cases, digital subtraction angiography (DSA) is required. Crossing lower pole renal vessel (s) or entrapment of the ureter by a vessel can prohibit urinary flow down the ureter. Vessels that wrap around the UPJ may be associated with obstruction or can be a product of renal dilation and hydronephrosis that distorts renal vascular architecture.

Case 1

A young man of age 20 years was operated upon twice--first time in Janauary 2000 and then in February 2001 after DTPA renogram showed recurrence of obstructive uropathy in left kidney. Again he had a follow up USG on 21 February 2005 which showed mild pelvicaliectasis in left kidney. There was a large lower polar vascular bundle pressing from front and causing a tight ureteropelvic junction obstruction (UPGO).(Fig.1)

Case 2

A girl of age 16 months had right-sided nephrostomy in Sept. 2004 and right-sided pyeloplasty on 26 Nov. 2004 for neonatal hydronephrosis. Follow up DTPA renogram on 3 March 2005 showed non-functioning right kidney and mild obstruction in left kidney, also seen in ultrasonography (8 Mega-Hertz). (Figs.2&3)

UPJ = Uretero Pelvic Junction
UPJO = UPJ Obstruction
VCUG = Voiding Cysto UrethroGram
UTI = Urinary Tract Infection

[1] Director & Chief Medical Officer, Centre for Nuclear Medicine and Ultrasound. Post Box # 16, Rangpur-5400, Bangladesh.

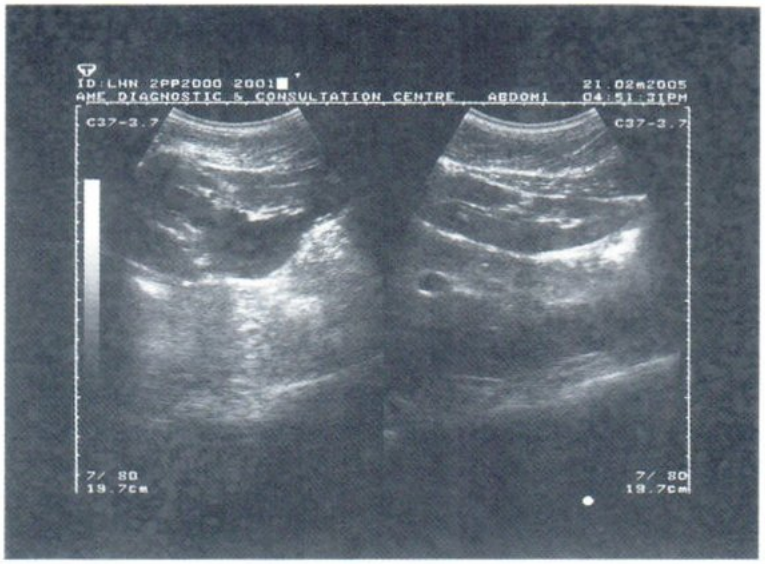

Fig.1 USG showing left hydronephrosis.

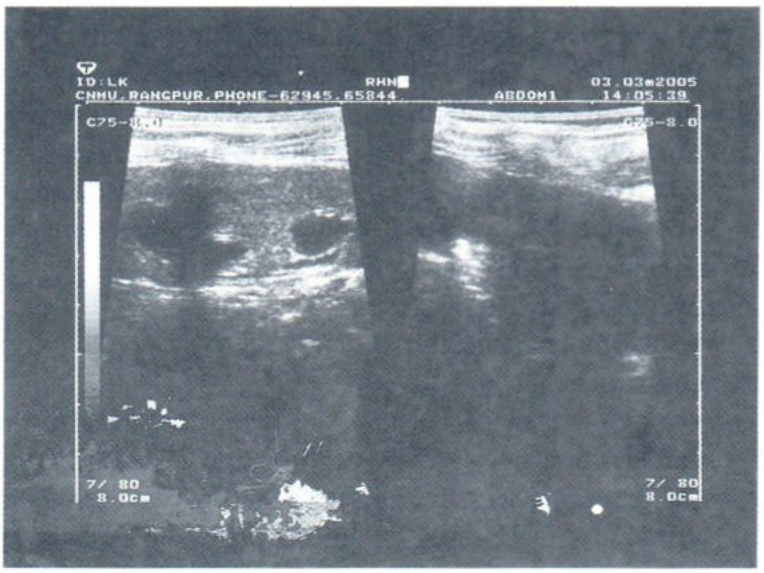

Fig.2 USG showing right hydronephrosis.

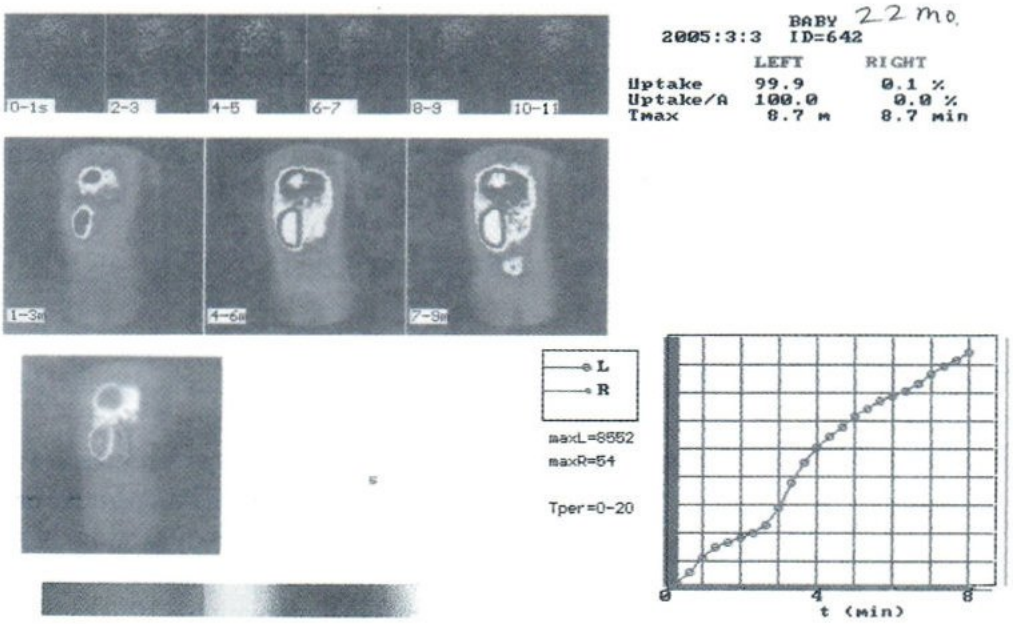

Fig.3 DTPA Renogram post pyeloplasty.

DISCUSSION

Neonates presenting with hydronephrosis should be fully evaluated with both a voiding cystourethrogram (VCUG) to rule out vesicoureteral reflux and a renal ultrasound soon after birth.These patients also should also be placed on prophylactic antibiotics (amoxicillin 15 mg/kg) to prevent urinary tract infections (UTIs), especially while diagnostic imaging is being obtained. If renal sonography demonstrates hydronephrosis without reflux on VCUG, a diuretic renal scan (mercaptoacetyltriglycine[MAG-3], diethylenetriamine pentaacetic acid [DTPA], or dimercaptosuccinic acid [DMSA] should be performed to quantify relative renal function and to define the extent of obstruction. Older chidren may present with UTIs, a flank mass, or intermittent flank pain secondary to a primary UPJ obstruction. Hematuria also may be a presenting sign if associated with infection. Adults can present with a variety of symptoms, including back and flank pain, UTI, and/or pyelonephritis. Through a detailed history, the pain may be correlated with periods of increased fluid intake or ingestion of a food with diuretic properties (ie, Dietl crisis). The goals in treating patients with UPJ obstruction are to improve renal drainage and to maintain or improve renal function. Dilation of the intrarenal collecting system or hydronephrosis does not necessarily imply obstruction. Specifically in children, renal pelvic dilation should be followed with serial imaging to assess for changes in dilation, renal parenchymal thickness and/or the pressence of scarring, and function. Surgical repair is indicated if a significant differential in serial imaging is present or if progressive deterioration of renal function occurs. Using this algorithm, patients with hydronephrosis are monitored closely with renal ultrasounds and renograms every 3-6 months. Similary, in adults, repair is recommended if ureteral obstruction is demonstrated on renal scan or intravenous pyelogram (IVP). The evaluation of an obstructed UPJ requires information about ureteral and surrounding anatomy, renal position and ectopy, associated vasculature, and renal function. Prior to surgical intervention, the surgeon frequently evaluates for

renal position/ectopy. mobility, and UPJ anatomy, such as high-insertion variants versus annular stricture variants. The major vascular supply of the UPJ comes from branches of the renal artery. These vessels usually lie in an anteromedial location in relation to the proximal urter. Aberant polar vessels also may be associated with the renal pelvis, causing compression and obstruction of the collecting system. These vessels arise from either the renal artery from a position proximal to the main intrarenal branching site or directly from the aorta. They can surround the UPJ and can be associated with obstruction, or they may be aberrantly positioned secondary to increasing hydronephrosis.[3]

CONCLUSION

We recommend sonography, nuclear medicine renography and other relevant imaging procedures in suspected UPJO before and after pyeloplasty.

REFERENCES

1. Stephens FD. Ureterovascular hydronephrosis and the aberrant renal vessels. J Urol 128: 984-987.1982.
2. Rouviere O. Lyonnet D, Berger P, Pangaud C. Gelet A, Martin X. Preoperative assessment of Ureteropelvic junction obstruction Helical CT as a replacement for DSA. Med Imaging International 10: 11 - 13, 2000.
3. Grasso M, et al. Ureteropelvic junction obstruction. eMedicine 2005.

SPLENIC ABSCESS IN WANDERING SPLEEN

Rutchanee PAISUWAN, M.D.[1]

The spleen is fixed in its position, in the left upper quadrant of the abdomen by suspensory ligament. Wandering spleen is a rare entity in which the spleen is attached by a long, vascular pedicle causing splenic hypermobility because of laxity or maldevelopment of its ligaments. Here is a report of one case of wandering spleen with complicated splenic abscess in a pediatric patient.

CASE REPORT

An eight-months-old child presented with abdominal distension, fever and nausea/vomiting after eating. Physical examination revealed an enlarged spleen (10 cm. below left costal margin). Laboratory investigation showed mild anemia (haemoglobin 9.8 g/dL, haematocrit 31.2%, peripheral smear-normocytic, mildly hypochromic anemia with lymphocytosis). Plain film shows no soft tissue shadow at splenic region which replaced by much overlying bowel gas (Fig.1). Computed tomography revealed no spleen at the normal location (Fig.2) but located at left mid-abdomen. The splenic hilum showed a whorled appearance with alternating high and low attenuation areas corresponding to enhancing vessels and fat respectively. Rim enhancing, low attenuation lesion, 7.5x3.5x5 cm. in size, is seen as ectopic spleen (Fig 3). Radiological diagnosis of splenic abscess secondary to torsion of wandering spleen was made. Emergency laparatomy found splenic torsion and abscess in the ectopic spleen, then splenectomy was done. The patient was discharged after an uneventful postoperative period.

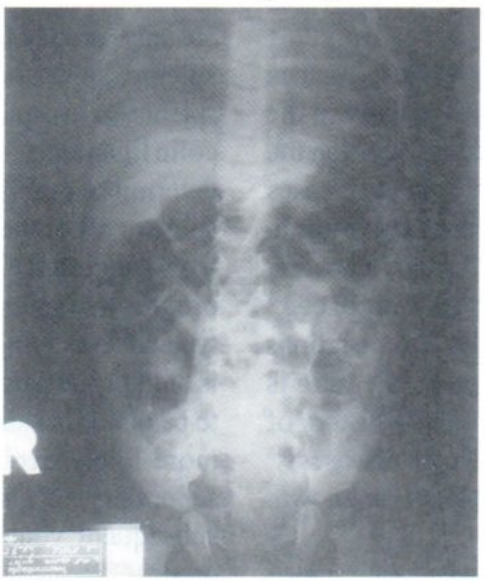

Fig. 1

[1] Department of Radiology, Vachira Phuket Hospital, Phuket, THAILAND 83000

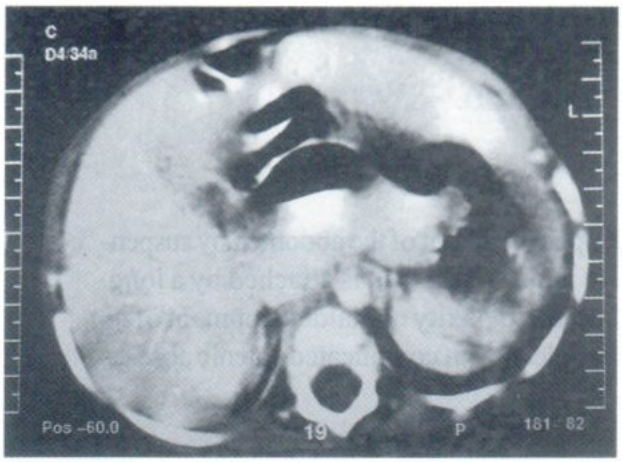

Fig. 2 No spleen is present in normal location.

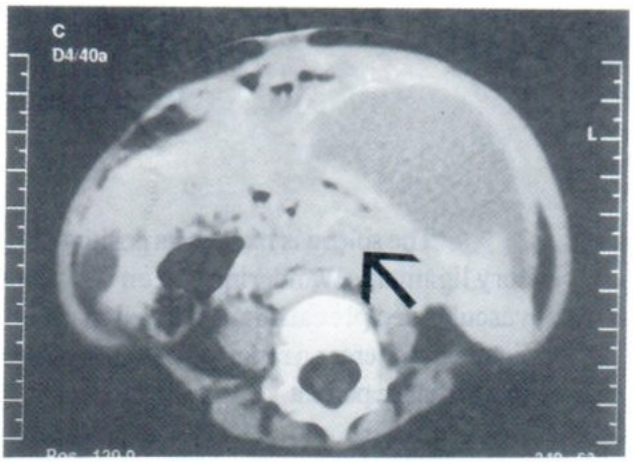

Fig. 3 Low-attenuating lesion in ectopic spleen and whorled appearance at splenic hilum (arrow)

DISCUSSION

Van Horne, a Dutch Physician, is credited with describing this condition in 1667 after performing an autopsy. In 1875, Martin, a German obstetrician, performed the first splenectomy for a wandering spleen. Ten years later, splenopexy was described and considered superior to splenectomy, a differential preference that changed several times over the years. Since Van Horne's discovery, approximately 400 cases of wandering spleen have been reported worldwide.

The incidence of wandering spleen is less than 0.2%.[1] Wandering spleen is rare, especially in the pediatric population. It usually occurs between the ages of 20 and 40 years, and 70% to 80% of cases are seen in women : most are of reproductive age at the time.[2] Children make up one third of all cases, and 30 % of them are younger than 10 years of age.[3] Under the age of 10 years, the male: female ratio is 1:1, but for those older than 10 years, the ratio is 1:7.[6-9] Some case reports have included a history of malaria, trauma, or benign hematologic diseases,[4-8] but the relationship to wandering spleen is unknown.

This variable incidence of wandering spleen according to age and sex can be explained by the two possible etiologies of this condition, which are acquired or congenital. The acquired form occurs in multiparous women as a result of hormonal changes during pregnancy. This causes a slackening of the abdominal wall and laxity of the ligaments normally attached to the spleen. In the congenital form, there is faliure of normal development of the dorsal mesogastrium when the lesser sac is formed. Therefore, attachments of the dorsal mesentery to the posterior peritoneum and diaphragm are faulty. In this form, suspensory ligaments of the spleen are not formed, or are only partially formed. These include the phrenicosplenic, splenorenal, phrenicocolic, pancreaticosplenic, gastrosplenic, splenocolic, and pancreaticocolic ligaments. The length of its vascular pedicle determines mobility of the spleen in the absence of some or all of these ligaments. Some case reports have suggested that wandering spleen is a result of progressive splenomegaly due to diseases such as typhoid fever, lymphoma, and especially malaria. This is unlikely because some wandering spleen is found to be of normal size or only moderately enlarged. A more likely explanation is that splenomegaly is secondary to chronic or recurrent torsion and subsequent venous congestion, not the primary process.[9-11]

Patients with wandering spleen may have an asymptomatic mass, a mass with abdominal pain, or

an acute abdomen. Sixty percent have a mass and pain. Acute torsion may precipitate fever, vomiting, and acute abdominal pain,[12] while recurrent, chronic torsion and detorsion may present as intermittent colicky pain, or vague abdominal discomfort.[13] Torsion can be precipitated by any movements of the body, changes in intra-abdominal pressure during respiration, or peristalsis or distention of adjacent organs.[10] Acute pancreatitis may be associated due to incorporation of the tail of the pancreas in the splenic vascular pedicle. Gastric compression or distension may also occur.[4,14]

Complication of wandering spleen includes infarction, gangrene, splenic abscess, variceal hemorrhage, and pancreatic necrosis.[14-17]

Given the rarity of wandering spleen and its nonspecific symptoms, early diagnosis is difficult. Some authors[18,19] suggest that the diagnosis can be made with certainty if the following criteria are met : (1) palpation of a mass with a notched edge; (2) mobility of the mass, which is painless in the left upper quadrant and painful in other directions ; (3) resonance on percussion in the left upper quadrant ; and (4) chronic intermittent pain. Wandering spleen can mimic several entities: tubo-ovarian abscess, ovarian cyst with torsion, uterine fibroid, urinary tract infection, acute appendicitis, intestinal obstruction, diverticulitis, colon cancer, cholecystitis. Laboratory values are often non-specific, however leucocytosis is generally present. Diagnosis of wandering spleen is very difficult with physical exam alone and often requires radiologic confirmation.

The diagnosis of wandering spleen can be confirmed radiographically, but there is still debate concerning which test is the most appropriate. Plain abdominal films may reveal a central abdominal mass with loops of bowel in the left upper quadrant. Barium enema may show a mass with medial and anterior displacement of the splenic flexure. Upper gastrointestinal tract studies may show an empty splenic fossa with a malpositioned stomach. Ultrasonography may show a solid mobile mass and absence of the spleen in the left upper quadrant. Doppler ultrasonography of the splenic vessels can be used to evaluate flow. Liver-spleen scans show splenic displacement, as well as the functional state of the spleen. In cases with torsion and ischemia, the spleen is absent and only the liver can be seen. CT of the abdomen may most often be suggestive of the diagnosis. Arteriography allows definitive evaluation of the splenic vasculture and signs of left-sided portal hypertension, if present.

Duplex ultrasonography and CT have gained popularity as the tests that can most easily and safely be used to diagnose wandering spleen. Ultrasonography may be limited by bowel gas or habitus, but one should be able to see and enlarged ectopic, hypoechoic mass with no flow in the splenic parenchyma (if torsion has occurred), decreased splenic arterial flow, and increased vascular impedance. CT shows wandering spleen and delineated other anatomic relationships. It may show absence of the spleen in its normal location, anterior to the left kidney and posterior to the stomach. The ectopic spleen can be seen as an abdominal or pelvic mass with an attenuation value lower than that of the normal spleen. Occasionally, ascites or necrosis of the pancreatic tail and torsion of the splenic vessels and surrounding fat (which appears whirled) can be seen. If torsion is chronic, a thick pseudocapsule is evident. The spleen is not enhanced by intravenous contrast medium if torsion has occurred and blood supply is lost.[4,10,13-16,20-21]

Definite treatment for wandering spleen is operative, since nonoperative treatment is associated with a complication rate as high as 65%. Complication of wandering spleen includes infarction, gangrene, splenic abscess, variceal haemorrhage, and pancreatic necrosis. Historically, splenectomy has been used for wandering spleen, but with increased understanding of the spleen's function, splenopexy with splenic salvage is now the procedure of choice in children. However, the decision to perform splenopexy versus splenectomy depends on both the timing of clinical presentation and the appearance and viability of the

spleen intraoperatively. In the emergent setting, the diagnosis of wandering spleen is usually made at laparotomy because patients present with an acute abdomen. The decision to perform splenpexy or splenectomy depends on the viability of the spleen after detorsion. If the spleen appears infarction, a splenectomy should be performed. Splenopexy is a reasonable option when the spleen appears viable after detorsion and the splenic vein is not thrombosed. Results of splenopexy are considered good.

CONCLUSION

Wandering spleen is a rare entity arising from the failure of fusion of the dorsal peritoneum. Splenic torsion should be recognized as a cause of an acute abdomen. Early diagnosis is difficult and is best done with a thorough clinical history, physical examination, and either duplex ultrasonography or CT. Definite treatment is surgical.

REFERENCES

1 Gore R, Levin M. Textbook of Gastrointestinal Radiology. 2nded. Philadelphia : WB Sauders; 2000: 1866-9.

2. Dawson JHM, Roberts NG : Management of the wandering spleen. Aost NZ J Surg 1994; 64: 441-444.

3. Allen KB, Andrews G : Pediatric wandering spleen. The case for splenpexy : review of 35 reported cases in the literature. J Pediatr Surg 1989; 24: 432-435.

4. Buehner M, Baker MS : the wandering spleen. Surg Gynecol Obstet 1992; 175: 373-387.

5. Bohrer J: Torsion of a wandering spleen; complicated by diaphragmatic hernia. Ann Surg 1940; 111 : 416-426.

6. Dowidar M : Wandering spleen : report of a case complicated by a traumatic cyst. Ann Surg 1949 ; 129 : 408-414.

7. Pollak E, Tesluk H : Volvulus of the spleen. JAMA 1977 ; 237 : 469-470.

8. Rosenthal L, Lisbona R, Banerjee K : A nucleographic and radiographic study of a patient with torsion of the spleen. Radiology 1974 ; 110 : 427-428.

9. Abell I : Wandering spleen with torsion of the pedicle. Ann Surg 1993 ; 98 : 722-735.

10. Lamesch, Lamesch A : Anomalies of the position of the spleen in the child.Langen becks Arch Chir 1993 ; 378 : 171-177.

11. Allen KB, Gay BB Jr , Skandalakis JE : Wandering spleen : anatomic and radiologic consideration. South Med J 1992 ; 85 : 976-984.

12. Cainzos M, Anigo F, Porto A, et al : Acute abdomen caused by torsion of the pedicle in a wandering spleen. Hepatogastroenterology 1993 ; 40 : 78-80.

13. Nemcek AA Jr, Miller FH, Fitzgerald SW: Acute torsion of a wandering spleen: diagnosis by CT and duplex Doppler and color flow sonography. Am J Radiol 1991; 157: 307-309.

14. Sheflin JJ, Lee CM, Kretchmar K: Torsion of wandering spleen and distal pancreas. Am J Radiol 1984 ; 142 :100.

15. Shiels WE, Johnson JF, Stephenson SR, etal: Chronic torsion of the wandering spleen. Pediatr Radiol 1989 ; 19 : 465-467.

16. Parker LA, Mittlestaedt CA, Mauro MA, et al: Torsion of the wandering spleen: CT appearance. J Comput Assist Tomogr 1984; 8: 1201-120

17. Angeras V, Almaskog B, Lukes P, et al: Acute gastric hemorrhage secondary to wandering spleen. Dig Dis Sci 1984 ; 29 : 1159.

18. Gindrey J, Piquard B : Volvulus de rate ectopique. Bull sou Med Afr 1966; 11 : 860-863.

19. Balik E, Yazici M, Tanelli C: Splenoptosis (wandering spleen). Eur J Pediatr Surg 1993; 3: 174-175.

20. Fujiwara T, Takehara Y, Isuda H, et al : Torsion of the wandering spleen : CT and angiographic appearance. J Comput Assist Tomogr 1995: 19: 84-86.

21. Herman TE, Siegel MJ : CT of acute splenic torsion in children with wandering spleen. Am J Radiol 1991 ; 156 : 151-153.

JUGULAR PHLEBECTASIS AND ACHALASIA CARDIA: A case report and review literature

Suporn JIANPERAPONG[1], Nitaya THONGSIBKAO[2]

ABSTRACT

Internal jugular vein phlebectasis and achalasia cardia were diagnosed in a 10 year -old boy. Chest film revealed posterior mediastinal mass. Ultrasonography of the neck showed fusiform dilatation of internal jugular vein and dilated esophagus. Esophagogram showed dilated esophagus with "Bird beak" or "Rat tail" appearance of distal part. The treatments of achalasia cardia were Heller's operation and esophageal dilatation and there was no treatment for phlebectasis.

Keywords: Phlebectasis, internal jugular vein, achalasia cardia, ultrasonography and esophagography.

INTRODUCTION

Internal jugular vein phlebectasis is an uncommon condition, defined as fusiform dilatation of internal jugular vein, usually idiopathic and asymptomatic. In this case we report internal jugular vein phlebectasia, which was occurred with achalasia cardia. The chest film, ultrasonography and esophagography were illustrated.

A CASE REPORT

A 10 year-old boy present with chronic vomiting and painless right neck mass for 2 years. This mass was increasing on straining or cough. The vomiting occur more prequently during swallowing liquid food than solid meal.

Physical examination showed a thin boy, with non-expansile cystic mass at right lower neck, anterior to sternocleidomastoid muscle. It was measured about 4 cm in diameter, and precipitating by cough, straining and Valsalva maneuver (Figure 1). Otherwise, it was unremarkable.

Fig.1 Photograph of a boy with right neck mass (*) **A:** Resting phase, **B:** The mass is increasing in size during straining.

[1, 2] Department of Radiology, Buddhachinnaraj hospital, Muang, Phitsanulok 65000, Thailand.

Chest film showed posterior mediastinum mass (Figure 4A).

Ultrasonogram revealed dilated right internal jugular vein, and increased more in size on Valsalva maneuver. (Figure 2) There was also dilated esophagus (Figure 3).

Esophagogram showed dilated entire esophagus, with gradual tapering end at distal part, seen as "rat tail" or "bird beak" appearance (Figure 4B and 5A-B)

The treatment was Heller's operation. The patient was slightly improved in a short time after operation, and there was recurrent vomiting, so dilatation of oesophagus have to be performed repeatedly.

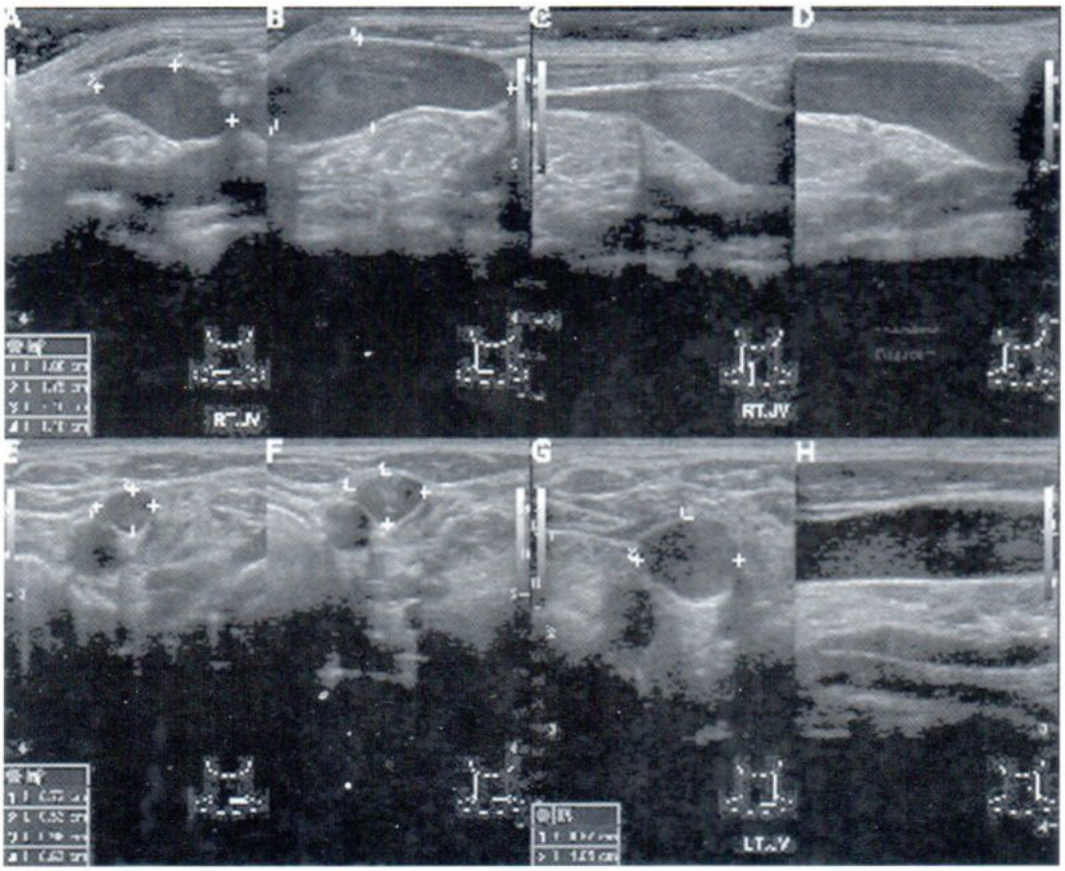

Fig.2 Ultrasonography of right (A-D) and left (E-H) internal jugular veins (caliper). Size of right IJV at rest (A-transverse, and C-longitudinal plane). It is more dilated during Valsalva maneuver (B and D), with the left IJV comparison (E-H).

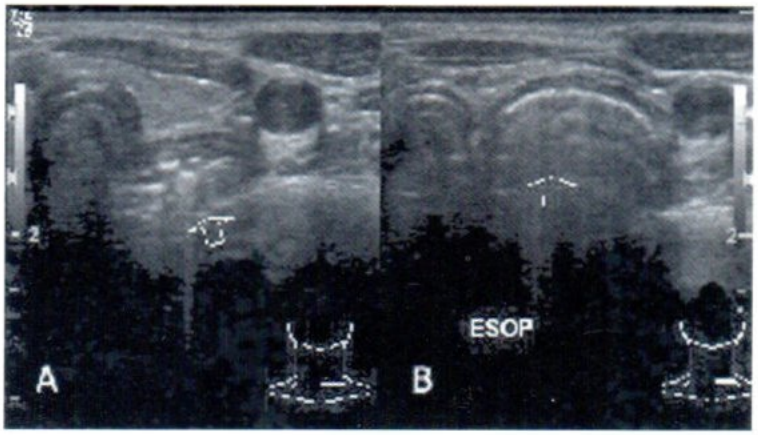

Fig. 3 At rest, air filled esophagus is noted at left side of trachea (arrow in **A**) and more dilated air-filled esophagus during Valsalva meneuver (arrow in **B**).

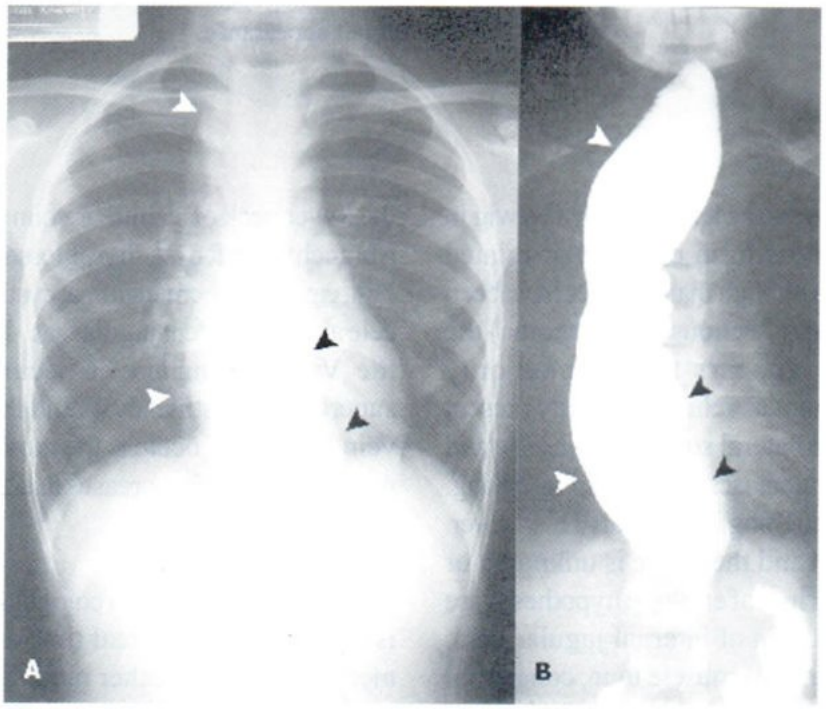

Fig. 4A Chest film shows posterior mediastinal mass (arrow head). Correlated frontal esophagogram **(B)** reveals dilated entire esophagus (arrow head).

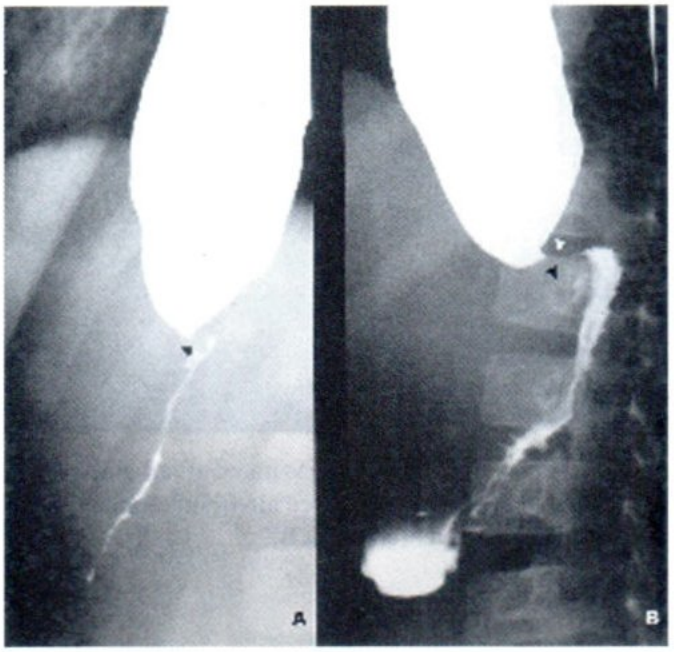

Fig. 5A, B Spot films of esophagogram show smooth tapering end of distal esophagus (arrow head) with bird beak or rat tail appearance.

DISCUSSION

Phlebectasis was the term used by Gerwig in 1952[1] to describe a fusiform or saccular dilated segment of the vein. Although many names have been used (venous aneurysm, venous cyst, venoma) the term phlebectasis appears to be commonly accepted.[2,3] Internal jugular vein is frequently present as a asymptomatic unilateral soft, non-palsatile and non-tender mass that increases with straining, crying, bending, sneezing, coughing and Valsalva maneuver. It is a rare condition and the cause is unknown or idiopathic.[2,4,5] The variety of etiology hypotheses are anomalous reduplication of internal jugular vein, increased scalenus anticus muscle tone, congenital origin, compression of the vein between the head of clavicle and the cupula, superior mediastinal irradiation, trauma, increased intrathoracic pressure and a congenital muscular defect in the wall of the vein.[2,3,5,6,7]

The differential diagnosis of a cystic mass in the lower neck of a child or young adult must include a branchial cleft cyst, thyroglossal duct cyst, dermoid cyst, cavernous hemangioma, cystic hygroma, laryngocele and a persistent jugular sac. The association with the Valsalva maneuver occurs in laryngocele, superior mediastinal cysts and the ectasia of jugular vein.[2,4,7] Laryngocele is the most common cause of neck mass, which increases in size with the Valsalva maneuver.[4,8]

Ultrasound with color Doppler flow imaging is the non-invasive, real time and best diagnostic method.[2,4,5,6,7] The other modalities used included computed tomography, venography, arteriography, nuclear scintigraphy and MRI.[2,6,7,8] Conservative management is generally recommended, but surgery may be advocated in cases of phlebitis, thrombus formation, rupture of the lesion or cosmetic deformity.[10]

Achalasia cardia was first described by Thomas Willis in 1674 . It is a condition, characterized by failure of relaxation of distal esophagus and esophagogastric junction. It could be primary, which there is absence of ganglion cells in the myenteric plexus or it could be secondary, which there is progressive degeneration of ganglion cells such as Chaga's disease. It is usually found in middle aged female, but uncommon in children.[12,13,14,15,16] Less than 5% of patients present before the age of 15 years.[11] Dysphagia is the most common presenting symptom in the patients with achalasia cardia. The child commonly presents with regurgitation, vomiting, recurring chest infection and rarely with respiratory distress and near miss sudden infant death syndrome.[11,14,16,17,18]

Diagnosis of achalasia cardia is based on history, barium swallowing, upper endoscopy and esophageal manometry. The esophagogram reveals dilated esophagus with smooth narrowing of the distal esophagus and esophagogastric junction, described as "bird beak" or "rat tail" appearance.[11, 12, 15, 16] As the degenerative neural lesion of this disease can not be corrected, the treatment is palliation of symptom and prevention of complications. The aims of treatment are improving of esophageal emptying time and decreasing in diameter of esophagus. The palliative treatments are pneumatic dilatation, Heller myotomy, pharmacotherapy and botulinum toxin injection.[11, 12, 17,19,20 ,21]

In the review literature, there is no previous report, mentioned that achalasia cardia occurs with jugular phlebectasis. This is the first report case of achalasia cardia, which there is dilated esophagus in the mediastinum and we think that is the cause of venous drainage obstruction, so there is resulting as dilatation of internal jugular vein.

In conclusion, although internal jugular phlebectasis is an idiopathic entity; we should look for the venous pathway obstruction as in this case.

ACKNOWLEDGEMENT

The authors would like to thank Assistant Professor Suwalee Pojchamarnwiputh; Department of Radiology, Chiengmai University, for her comment and Mr. Don Chiasson for reviewing the manuscript.

REFERENCE

1. Gerwig WJ.Internal jugular phlebectasia.Ann Surg 1953; 135:130-3
2. Paleri V, Gopalakrishnan S. Jugular phlebectasia: theory of pathogenesis and review of literature. Int J Pediatr Otorhinolaryngol. 2001; 57(2): 155-9.
3. Al-Shaikhi A, Kay S, Laberge JM. External jugular venous aneurysm: an unusual cause of a neck mass in a young child. J Pediatr Surg. 2003; 38(10):1557-9.
4. DKK Ng, KL Kwok, HS Lam. Unilateral internal jugular phlebectasia. HKMJ 2000;6: 431
5. Jeon CW, Choo MJ, Bae IH, Shin SO, Choi YS, Lee DW, Sim KH. Diagnostic criteria of internal jugular phlebectasia in Korean chidren. Yonsei Med J. 2002; 43(3):329-34.
6. Rajendran VR, Vasu CK, Regi George AN, Anjay MA, Anoop P. Unilateral internal jugular phlebectasia. Indian J Pediatr. 2004; 71(8): 751-3.
7. Fan XD, Qiu WL, Tang YS. Internal jugular vein phlebectasia: case report. J Oral Maxillofac Surg. 2000; 58(8):897-9.
8. Sander S, Elicevik M, Unal M, Vural O. Jugular phlebectasia in children: is it rare or ignored? J Pediatr Surg. 1999 ; 34(12):1829-32
9. Yildirim I, Yuksel M, Okur N, Okur E, Kylic MA. The sizes of internal jugular veins in Turkish children aged between 7 and 12 years. Int J Pediatr Otorhinolaryngol. 2004; 68(8): 1059-62.

10. Rossi A, Tortori-Donati P. Internal jugular vein phlebectasia and duplication: case report with magnetic resonance angiography features.: Pediatr Radiol. 2001; 31(2):134.
11. Choudhury SR, Singh D, Debnath P R, Gupta N. Achalasia cardia in an infant. http://bhj.org/journal/2004_4602_april/html/achalasia_201.htm
12. Ott DJ. Motility disorders of the esophagus. In: Gore RM, Levine MS. Text book of gastrointestinal radiology. Philadelphia: Saunders, 2000: 319-322
13. Rattan KN, Sharma A. Achalasia cardia. Indian J Pediatr 2000; 67 (2) : 157-58.
14. Icagasioglu D, Tanzer F, Gultekin A, et al. Childhood achalasia. Turk J Pediatrl 1996; 38 (3) : 385-88.
15. Woodfield CA, Levine MS, Rubesin SE, et al. Diagnosis of primary versus secondary achalasia; reassessment of clinical and radiographic criteria. Am J Roentgenol 2000; 175 (3) : 727-31.
16. Patil KK, Telmesani A, Ogunbiyi OA. Childhood Achalasia -a case report. West Afr J Med 1993; 12 (3) : 172-74.
17. Thomas RJ, Sen S, Zachariah N, Chacko J, Mammen KE. J R Coll Surg Edinb Achalasia cardia in infancy and childhood: an Indian experience. Thomas RJ, Sen S, Zachariah N, Chacko J, Mammen KE. J R Coll Surg Edinb. 1998; 43(2):103-4.
18. Sarin YK, Stephen E. Achalasia cardia in an infant. Indian Pediatr. 1997 ;34(3):251-4.
19. Eckardt VF, Gockel I, Bernhard G.Pneumatic dilation for achalasia: late results of a prospective follow up investigation.Gut. 2004 ;53(5): 629-33
20. Cheng YS, Li MH, Chen WX, Chen NW, Zhuang QX, Shang KZ. Selection and evaluation of three interventional procedures for achalasia based on long-term follow-up. World J Gastroenterol. 2003; 9(10): 2370-3.
21. Ghoshal UC, Kumar S, Saraswat VA, Aggarwal R, Misra A, Choudhuri G. Long-term follow-up after pneumatic dilation for achalasia cardia: factors associated with treatment failure and recurrence. Am J Gastroenterol. 2004; 99(12):2304-10.

PANCREATIC CANCER: IN TRANG HOSPITAL 2001-2004

Daranee PITANUPONGSA, M.D.[1]

ABSTRACT

Pancreatic adenocarcinoma is the second most common cause of death from cancer of the gastrointestinal tract. Due to the absence of early signs or symptoms, many patients were diagnosed after the cancer is too advanced for surgical removal.

Demographic data, clinical presentation, sonography and computed tomography (CT) features of eight patients with pancreatic cancer, diagnosed in Trang Hospital between January 2001 and December 2004 were reviewed.

The patients were five men and three women with age ranging from 32 to 77 years old (mean age, 51.4 years). All patients presented with obstructive jaundice. All of the cases, the cancer were localized to the head of the pancreas. Direct visualization of the tumor by sonography was about 83% and by CT was 100% Six cases (75%) were hypovascular masses. Dilatation of both the pancreatic duct and the biliary ducts were observed in all patients by CT. All cancer were unresectable due to vascular encasement. Three cases (37.5%) had liver metastases.

Key words: pancreatic cancer, pancreatic adenocarcinoma

INTRODUCTION

Of all the GI malignancies, pancreatic adenocarcinoma is the second most common cause of death from cancer. In clinical practice, pancreatic cancer is synonemous with pancreatic ductal adenocarcinoma, which constitutes 90% of all primary malignant tumor arising from the pancreatic gland.[3] Clinical symptoms and signs develop late and depend on the site of the tumor. Tumors in the body and tail produce late symptoms. Carcinomas of the pancreatic head typically present with obstructive jaundice. This presentation usually leads to either abdominal ultrasound or computed tomography scan to determine the source of the symptoms. Due to the absence of early signs or symptoms, many patients are diagnosed only after the disease has already spread or metastasized which means the cancer is too advanced for surgical removal.[1-5] The purpose of this study was to identify abdominal sonography and CT features of the pancreatic cancer diagnosed in Trang Hospital.

MATERIALS AND METHODS

The patients of pancreatic cancer diagnosed in Trang Hospital between January 2001 to December 2004, were reviewed retrospectively. Patients demographic data, clinical presentation, sonography and computed tomography (CT) features were analyzed.

[1] Section of Radiology, Trang Hospital, Trang, 92000 Thailand

RESULT

The patients were five men and three women, 32-77 years old (mean age, 51.4 years). The symptoms of all eight patients were obstructive jaundice.

Six of the eight patients had abdominal ultrasonographic study to be reviewed. Dilatation of the common bile duct was observed in all six patients and dilatation of the pancreatic duct was observed in three patients. Of the six patients, hypoechoic mass was observed in the head of the pancreas in five patients, but no mass was observed anywhere in one patient. Calcification was observed in the mass in one patient. (Fig.1 and 2)

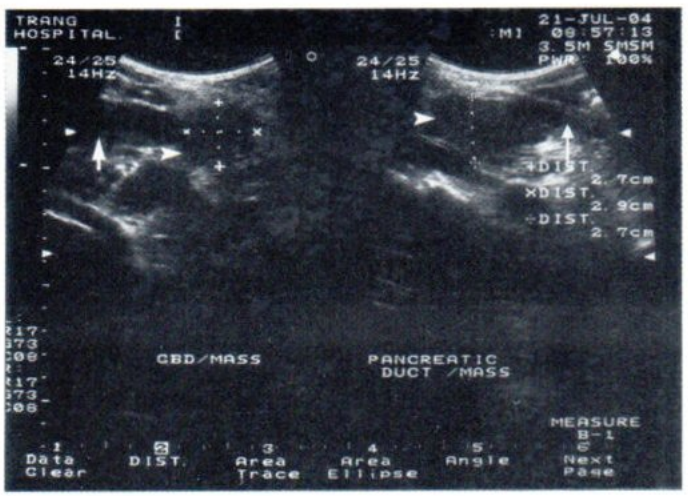

Fig.1 66-years-old man with mass in pancreatic head.
Sonography shows hypoechoic mass in pancreatic head (arrowhead) with obstruction of common bile duct (short arrow) and pancreatic duct (long arrow).

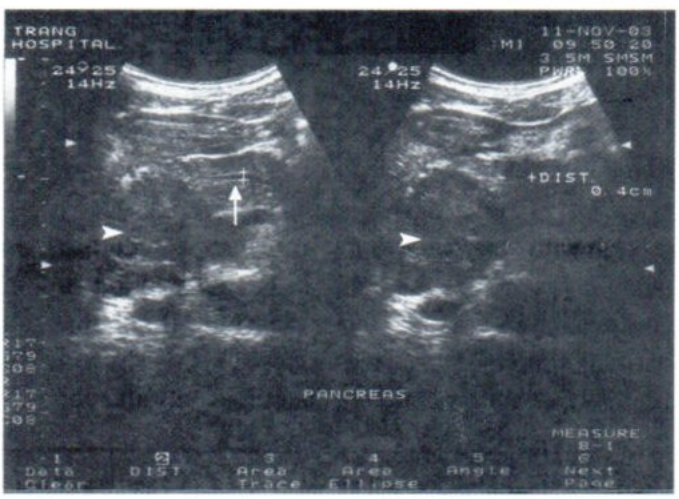

Fig.2 37-years-old man with mass in pancreatic head.
Sonography shows hypoechoic mass in pancreatic head (arrowhead) with obstruction of pancreatic duct (long arrow).

All eight patients underwent CT (Tomoscan SR 7000, Philips Medical Systems) of the upper abdomen. Pancreatic mass was observed in all patients. All of them were localized to the head of the pancreas and one had alrealy expanded to the body of the pancreas. The size of the masses were about 3 to 8 cm(mean size, 4.7 cm.). Six pancreatic masses showed hypovascular and one mass had internal calcification same as sonographic feature. The other two masses exhibited heterogeneous enhancement (one had opened biopsy from other hospital before underwent CT and another one was the biggest lesion). Obstruction of the main pancreatic duct and common bile duct were observed in all eight patients. The major blood vessels involved by the mass were detected in all patients. Three cases had liver metastases. (Fig.3 and 4)

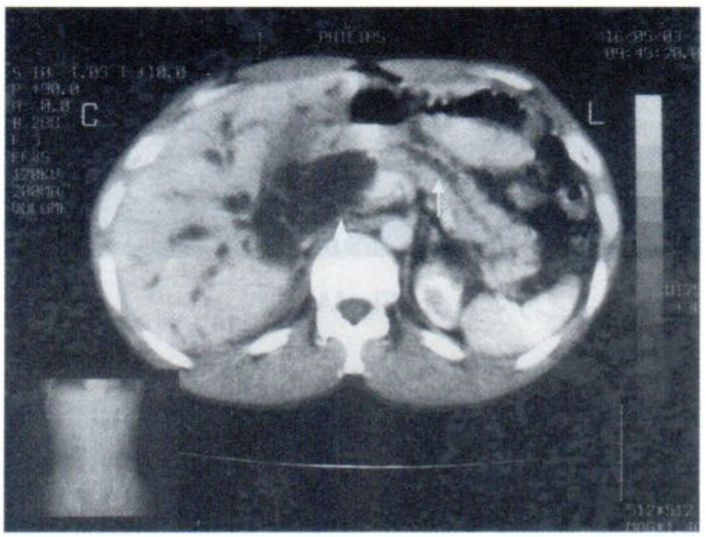

Fig. 3A

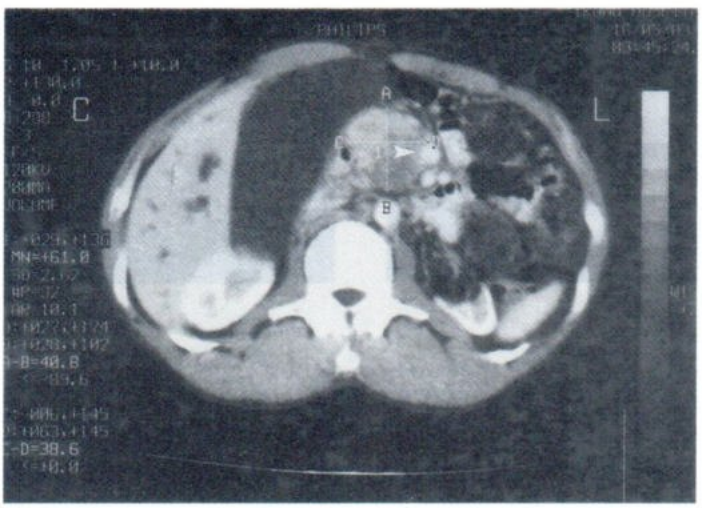

Fig. 3B

Fig.3 42-years-old man with mass in pancreatic head.
A. On contrast-enhanced CT, the pancreatic duct (long arrow) and biliary ducts (short arrow)are dilated.
B. More caudally, the tumor is seen in the region of pancreatic head and irregularity of the superior mesenteric vein (arrowhead) at the point of contact with the tumor.

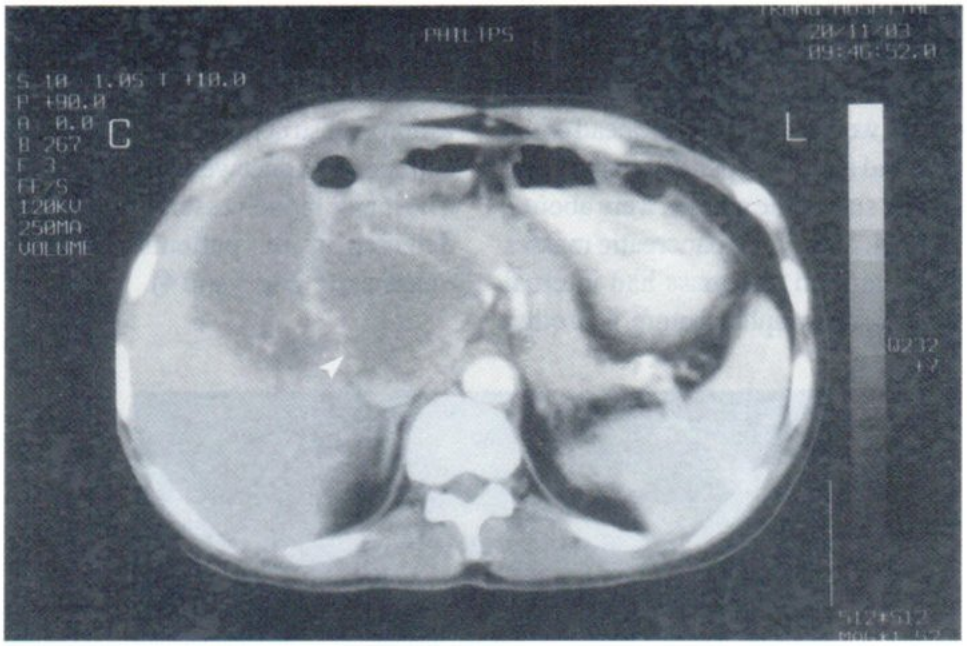

Fig.4A

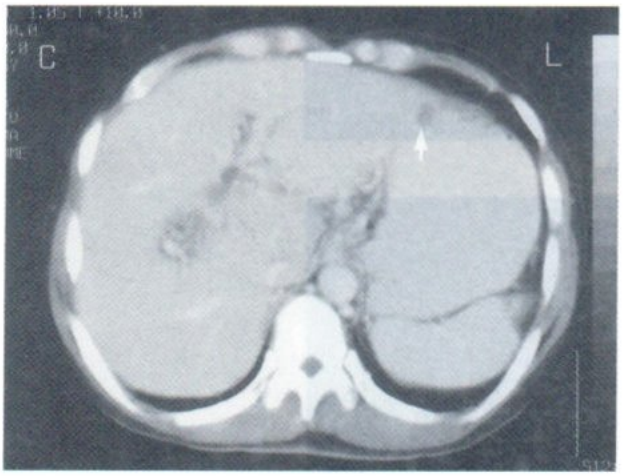

Fig.4B

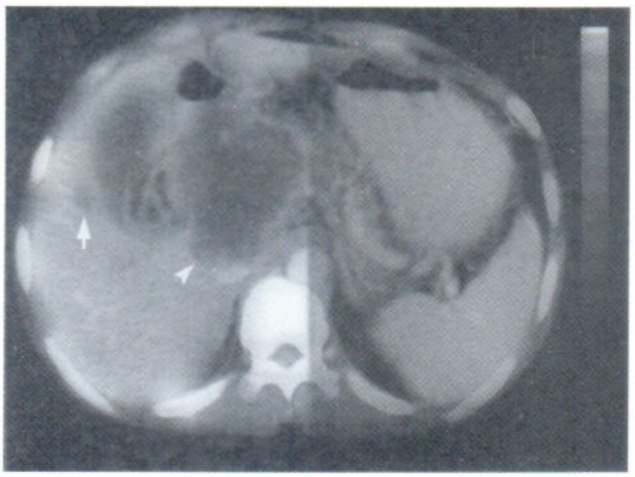

Fig.4C

Fig.4 37-years-old man with mass in pancreatic head.
On contrast-enhanced CT in arterial phase (A) and portal venous phase (B and C), hypovascular mass (arrowhead) is seen in the region of pancreatic head. Two hepatic metastases (short arrow) are also observed.

DISCUSSION

In this series, it was found that the disease is more common in men than in women the same as described in the previous literatures.[1,2,3,5,14] The male: female ratio was about 1.67: 1. The majority of cases were diagnosed between the ages of 60 and 80. It is uncommon in those younger than 40 years.[1,3,14] But in my series, the average age was about 51.4 years lower than all previous literatures. Two patients (25%) were younger than 40 years (32 and 37 years old) and both were male. All of the cases, the cancer were localized to the head of the pancreas which is mostly the location of the disease and typically presented with obstructive jaundice.[1-4] Imaging often begins with transabdominal sonography to identify the cause of jaundice. Sonography can screen for the presence and the point of common bile duct obstruction. However, The presence of obscuring overlying bowel gas and the variable skill of the operator limit the sensitivity of this technique for identification and staging of the pancreatic tumors. After sonography, CT is the modality mostly used as the primary modality for diagnosis and staging.[2] In this series, direct visualization of the tumor by sonography was about 83% but by CT, all tumors (100%) were visualized in all cases. The masses were about 4.7 cm. in average diameter. Most lesions (75%) were hypovascular. Ductal dilatation occurred in all patients and all had dilatation of both the pancreatic ducts and the biliary ducts. Vascular encasement usually determines unresectability[2,8,9,11,12] and was seen in all cases in this series. The liver, peritoneum and regional nodes are the organs most commonly involved by distant metastases in patients with pancreatic carcinoma. 60% of the patients who present with pancreatic ductal adenocarcinoma have advanced diseases. CT has been reported a sensitivity of 75-87% for liver metastases.[2] In this series, it was found that liver metastases had already presented in 3 of the 8 cases (37.5%). The identification of nodal and peritoneal disease is difficult with all imaging modalities.[2] And in this series, the regional node metastases and peritoneal implants were not visible.

CONCLUSION

It was found that all pancreatic cancer diagnosed in Trang Hospital were unresectable at the time of initial diagnosis. Two of the eight patients were younger than 40 years. In all cases, the cancer were located in the head of the pancreas and typically presented with obstructive jaundice. Sonography was less sensitive than CT for the identification of the pancreatic mass. Due to initial symptoms of the pancreatic cancer are usually nonspecific e.g. abdominal pain and weight loss, 80-90% of patients have regional and distant metastases by the time they were diagnosed. I, therefore, suggest the use of sonography as a screening examination and CT as a detail study in the evaluation of the patient presenting with nonspecific symptoms such as abdominal pain and weight loss.

REFERENCE

1. Gore RM, Levine MS. Textbook of Gastrointestinal Radiology. 2 nd ed. Philadelphia: W.B. Saunders Company; 2000. P.1796-1801.
2. Tamm EP, Silverman PM, Charnsangavej C, et al. Diagnosis, Staging, and Surveillance of Pancreatic Cancer. AJR Am J Roentgenol [serial online] 2003 May [cited 2005 Feb 5]: 180 (5): [19 screens]. Available from: URL: http://www.ajronline.org/cgi/content/full/ 180/ 5/1311.
3. Neelala Anand MK, Boylan C, et al. Pancreas, Adenocarcinoma. Medicine Instant Access To the Minds of Medicine [medline] 2004 March [cited 2005 Mar 10]. Available from: URL: http: //www.emedicine. com/radio/topic 516.htm.
4. Bottger TC, Boddin J, Duber C, et al. Diagnosis and staging of pancreatic carcinoma-what is necessary ? Oncology 1998; 55: 122-129.
5. Aladar P. Pancreatic Head Mass: What can Be Done ? Diagnosis: Surgery. JOP. J Pancreas (online) 2000; 1 (3 Suppl.): 127-129.

6. Landis SH, Murray T, Bolden S, et al. Cancer statistics. CA Cancer J Clin 1999; 49: 8-31.
7. Yassa NA, Yang J, Stein S, et al. Gray-scale and color flow sonography of pancreatic ductal adenocarcinoma. J Clin Ultrasound 1997; 25: 473-480.
8. Freeny PC, Marks WM, Ryan JA, et al. Pancreatic ductal adenocarcinoma: diagnosis and staging with dynamic CT. Radiolog 1988; 166: 125-133.
9. Diehl SJ, Lehmann KJ, Sadick M, et al. Pancreatic cancer: value of dual-phase helical CT in assessing resectability. Radiology 1998; 206: 373-378.
10. Prokesch RW, Chow L, Beaulieu CF, et al. Isoattenuating Panereatic Adenocarcinoma at Multi-Detector Row CT: Secondary signs. Radiology 2002; 224: 764-768.
11. Coley SC, Strickland NH, Walker JD, et al. Spiral CT and the preoperative assessment of pancreatic adenocarcinoma. Clin Radiol 1997; 52: 24-30.
12. Imbriaco M, Megibow AJ, Camera L, et al. Dual-Phase Versus Single-phase Helical CT to Detect and Assess Resectability of Pancreatic carcinoma. AJR 2002 ; 178 : 1473-1479.
13. Freeny PC, Traverso LW, Ryan JA. Diagnosis and staging of pancreatic adenocarcinoma with dynamic computed tomography. Am J Surg 1993; 165: 600-606.
14. Morrison BJ. Prevention of pancreatic cancer. The U.S. Preventive services Task Force, 1993.

UTERUS DIDELPHYS, OBSTRUCTED HEMIVAGINA AND IPSILATERAL RENAL AGENESIS, 2-CASE REPORT.

Teerachai LEELAMETAKUL M.D.[1]

ABSTRACT

Two female teenagers with progressive dysmenorrhea were sent to tertiary care unit for further management of the pelvic masses which erroneously given preliminary diagnosis to be endometriotic disease and pelvic abscess. Following thoroughly review of clinical data and imaging studies, the patients showed to have double uterus, obstructed hemivigina and absent right kidney. The pelvic mass, thus, represented hematocolpos and hematometra. Resected vaginal septum is the treatment of choice and should be performed earlier, to prevent gynaecologic complications and improve reproductive outcome. Non invasive imaging techniques may have the important roles in the diagnosis of intrapelvic mass in female adolescence with absent kidney which could be the consequence of developmental uterine anomalies.

INTRODUCTION

The definite association of uterus didelphys, obstructed hemivagina and ipsilateral renal agenesis was documented in the literature since 1922 by Purslow.[1] Rock and Jones found a more common occurrence of this complex anomalies on the right side.[2] Uterus didelphys with obstructed hemivagina is the extreme spectrum of defective fusion of paramesonephric (Mullerian) duct and derivative thereof. Because of accompanying growth with the mesonephric (Wolffian) duct, renal anomaly always comes about together. Both cases had been misdiagnosed by referring physicians to be endometriotic diseases and pelvic abscess and were sent for further management.

2-CASES REPORT

CASE1: 15 year old female with lower abdominal mass

This female adolescent experienced dysmenorrhea since her first menstruation. The symptom became progressive and brought her to a private hospital. Initial transabdominal US exhibited two right adnexal masses with absence of right kidney at the native site. She was further investigated by intravenous urography (fig.1) and abdominal CT scan (fig.2,3). These were concluded to be right endometriotic cyst and right pelvic kidney. The patient was sent to tertiary care hospital for further treatment. Following transabdominal US by gynecologic ultrasonologist, it was found that these two right adnexal masses could be hematocolpos and hematometra (fig.5,6). No right kidney was found. Subsequent vaginal exam during narcosis noted that she had obstructed right hemivagina. The patient received surgical treatment by vaginal septum resection for ample drainage of hematocolpos and exposing the cervix. Final diagnosis was uterus didelphys with obstructed right hemivagina and ipsilateral renal agenesis.

[1] Department of Radiology, Songkhla general hospital, Songkhla, THAILAND 90100

CASE 2: 12 year old female with right sided abdominal pain

The patient was referred from a general practioner clinic for a suspicion of pelvic abscess. She had a history of severe dysmenorrhea since the menarche and last more than one day. On her initial transabdominal US, a well demarcated hyperechoic mass was shown. This was contiguous with uterus which appeared to be hydrometra and markedly deviated to the right side. A smaller left sided uterine-like structure was also found. Further lower abdominal CT scan was performed and obviously showed the obstructed right vagina causing hematocolpos and hematometra (fig.6,7). This patient also had absent right kidney as well (fig.8). All findings were supportive for the diagnosis of uterus didelphys with obstructed right hemivagina.

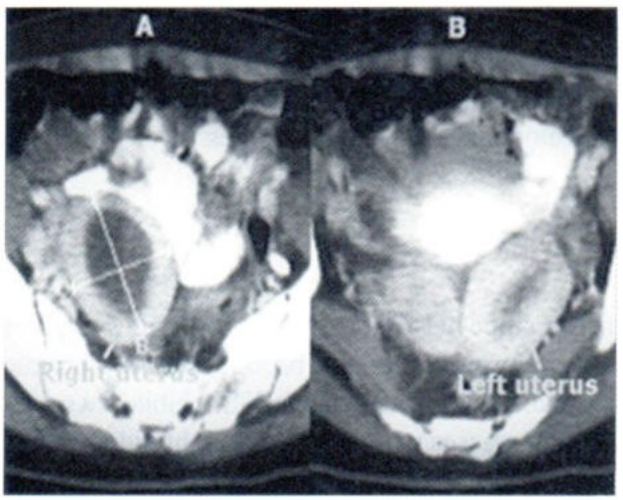

Fig.1

Fig.2

Fig.1-2 Sequential slices of the 15-year-old female with uterus didelphys and obstructed right hemivagina clearly unveil hydrometra of right sided uterus(A), smaller nonobstructed left sided uterus(B) and right sided hematocolpos(C).

Fig.3 Intravenous urography of the 15-years-old female shows no right renal pyelogram. Opacity in lower abdomen from previous oral contrast administration for previous abdominal CT is noted.

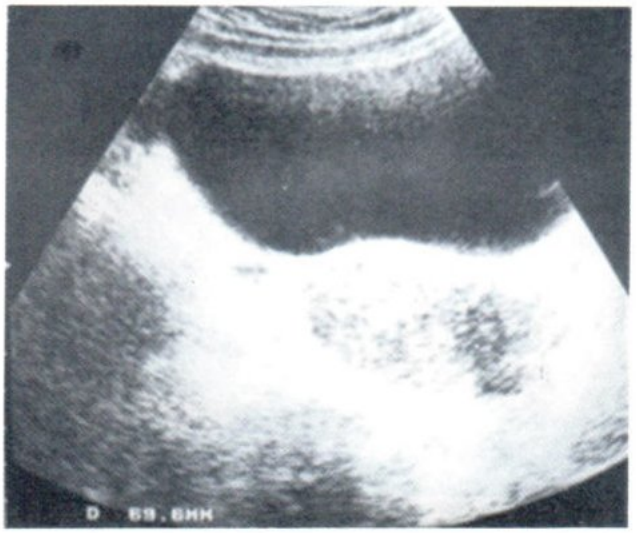

Fig.4 Left oblique sagittal scan shows left sided uterus.

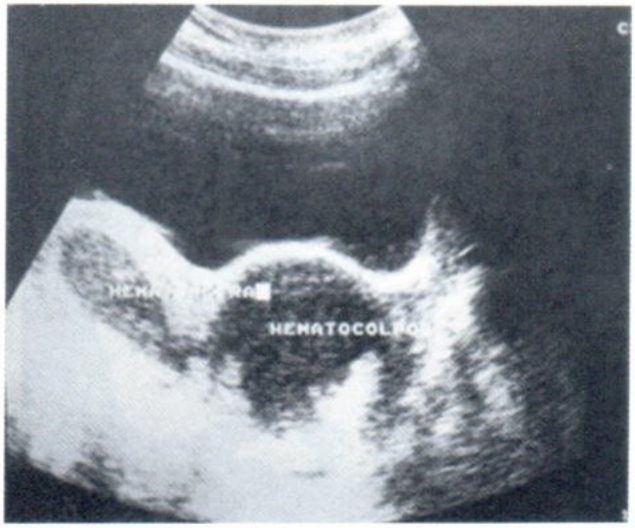

Fig.5 Right oblique sagittal scan shows hematometra and hematocolpos of right sided uterus and obstructed right hemivagina.

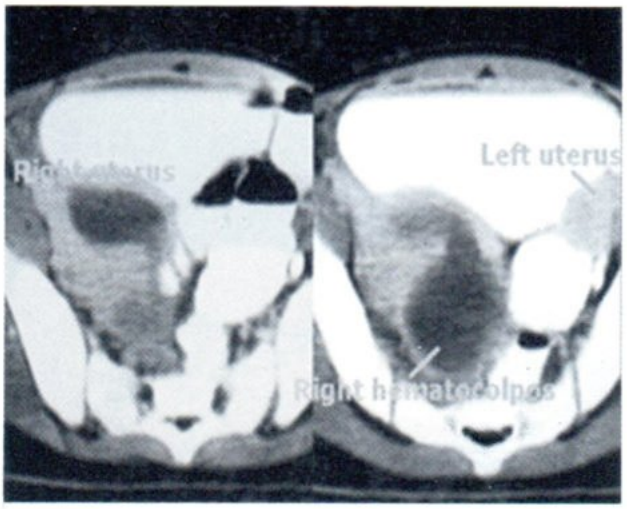

Fig.6

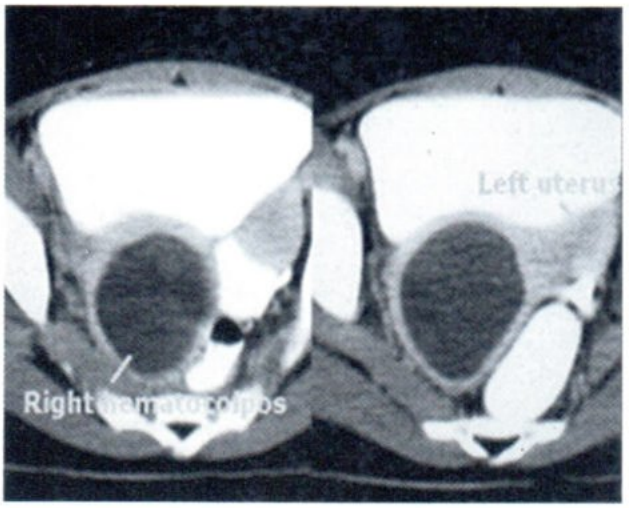

Fig.7

Fig.6-7 Lower abdominal cuts of the 12-years-old female shows mild right hematometra and marked right hematocolpos. Smaller left uterine-like structure is also observed. Note the content of hematocolpos appeared clearer than the first patient, suggestive of less chronicity.

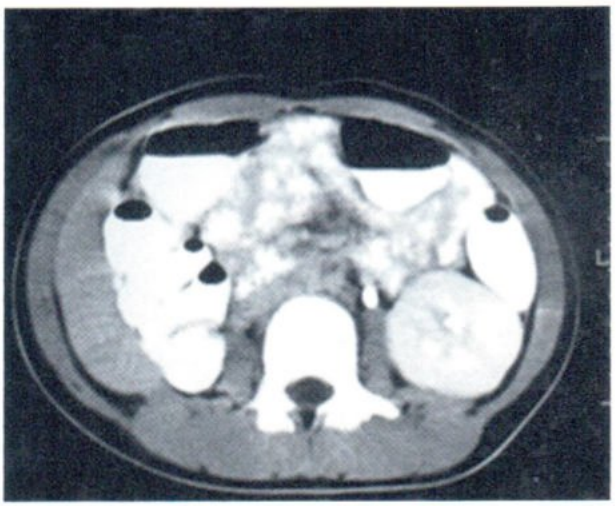

Fig.8 Higher level cut of the 12-years-old female shows absence of the right kidney in the right renal fossa.

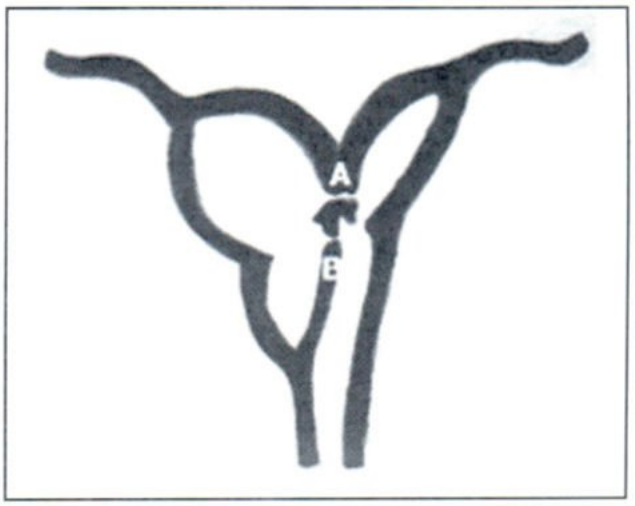

Fig.9 Diagrammatic illustration for both patients' mullerian anomalies shows association of uterus didelphys, obstructed hemivagina and ipsilateral renal agenesis. Communicated sites between the two uteri may occur either above the internal cervical ora (A), or anywhere at the level of the vagina (B).

DISCUSSION

The clinical syndrome comprising of double uterus, obstructed hemivagina and ipsilateral renal agenesis, is suggestive of an embryonic arrest occurring between 8th and 12th week of pregnancy that simultaneously affect the Mullerian and metanephric ducts.[3] Patients may be asymptomatic until menarche. Obstructive symptoms may present with progressive dysmenorrhea, lower abdominal mass or chronic vaginal discharge depending on degree of obstruction and presence of communication connection the right and left sides of Mullerian system at the level of vagina or above internal cervical ora (fig.9).[4]

Manifestations of the fusion defect ranges from uterus didelphys to arcuate uterus which uterine fundus is somewhat indented in the center. The most common form is bicornuate uterus in which the uterus has two cornua connected at their caudal ends.[5] Fusion failure also results in longitudinal vaginal septa which can cause a complete double vagina and found in up to 57% of cases.[6,7,8] If one of the vaginal outlet is not utterly developed, obstructive symptoms of hematocolpos and hematometra will occur. Longitudinal vaginal septum is very common in the case of uterus didelphys as we encountered in these reported cases.

Double uterus with blind hemivagina may be the consequence of damage to the caudal portion of the Wolffian duct. From embryologic viewpoint, while the cephalic portions of Mullerian and Wolffian ducts are divided by mesenchyma, more caudally the anatomic relations become closer; however they continue to present different morphologic pictures of interactions between epithelium and interstitial tissue which brought about the differentiation of the two ducts.[9] These findings, according to which development of the Mullerian duct may be inhibited by a defective Wolffian duct, support evidence that the former duct uses the latter duct to lead its descent toward urogenital sinus.[10] Hence, the frequent associated urinary tract anomaly is detected.

Awareness of this syndrome should be lead to its prompt diagnosis. This in turn should allow for early and suitable surgical management for decreasing the complications such as hematosalpinx, pyosalpinx, pyocolpos,[4,11] endometriosis,[12] intrapelvic adhesions[4] and can improve reproductive outcome.13 If proper treatment has been considerably delayed, hemihysterectomy with or without salpingo-oophorectomy may become necessary.

In view of the fact that the age group of the presented patients was teenage. Vaginal exam or other invasive methods e.g. hysterosalphingography may be prohibited. Non invasive imagings are more favoring in abnormality detections. Nowadays, transabdominal US is frequently the method of choice. If this provides insufficient anatomical details, CT may be more informative. Appropriate imaging procedures would save the patient from unnecessary further mostly invasive examinations and/ or surgical interventions e.g. laparoscopy or hysteroscopy. Even though, no matter what imaging performed, basic knowledge of developmental urogenital system is needed.

SUMMARY

Radiologists ought to concern hematocolpos or hematometra from developmental Mullerian anomaly in the differentials diagnosis of the young adult female pelvic masses. And if this is inconspicuity, additional detection of the associated anomalies, in particular, the urinary tract must be done. One must know that there may have been other Mullerian anomalies that did not come to light; that is because of many woman have no leading symptoms as mentioned above.

REFERENCES

1. Purslow CE. A case of unilateral hematocolpos, hematometra and hematosalpinx. J obstet Gynaecol Br Emp 1922;29:643.

2. Rock JA, Jones HJ. The double uterus associated with an obstructed hemivagina and ipsilateral renal agenesis. Am J Obstet Gynecol 1980;138:339-42.
3. Candiani GB, Fedele L, Candiani M. Double uterus, blind hemivagina and ipsilateral renal agenesis: 36 cases and long-term follow-up. Obstet Gynecol 1997;90:26-32.
4. Jacques PS, Theodore CN, Konald AP et al. Uterus didelphys, obstructed hemivagina and ipsilateral renal agenesis: the university of Minnesota experience. Fertil steril 1992: 57; 756-61.
5. Golan A, Langer R, Rukovsky I et al. Congenital anomalies of the Mullerian system. Fertil Steril 1989;51:747-55
6. Rock JA, Schlaff WD. The obstetric consequences of uterovaginal anomalies. Fertil Steril 1985;43:681-92.
7. Heinonen PK, Saarikoski S, Pystynen P. Reproductive performance of woman with uterine anomalies, an evaluation of 182 cases. Acta Obstet Gynecol Scand 1982;61:157-62.
8. Buttram VC Jr. Mullerian anomalies and their management. Fertil Steril 1983;40:159-63.
9. Marshall FF, Beisel DS. The association of uterine and renal anomalies. Obstet Gynecol 1978;51:559-62.
10. Acien P. Embryological observations on the femal genital tract. Hum Reprod 1992;7:437-45.
11. Rock JA, Thompson JD. Surgery for anomalies of the mullerian ducts. In: Te Linde's operative Gynecology 7th edn, Philadelphia: J.B. Lippincott, pp. 628-46.
12. Olive DL, Henderson DY. Endometriosis and mullerian anomalies. obstet Gynecol 1987; 69:412-15.
13. Stein AL, March CM. Pregnancy outcome in woman with mullerian duct anomalies. L Reprod Med 1990;35:411-4.